DEUTSCHES ELEKTRONEN-SYNCHROTRON DESY

DESY 85-005
January 1985

CORRELATIONS AND STATIC ENERGIES IN THE STANDARD HIGGS-MODEL

by

I. Montvay

Deutsches Elektronen-Synchrotron DESY, Hamburg

ISSN 0418-9833

NOTKESTRASSE 85 · 2 HAMBURG 52

To be sure that your preprints are promptly included in the
HIGH ENERGY PHYSICS INDEX ,
send them to the following address (if possible by air mail) :

DESY
Bibliothek
Notkestrasse 85
2 Hamburg 52
Germany

DESY 85-005
January 1985

ISSN 0418-9833

Correlations and static energies in the standard Higgs-model.

I. Montvay
Deutsches Elektronen-Synchrotron DESY, Hamburg

Abstract: Correlations in the W-boson and Higgs-boson channels and the static energy of an external SU(2)-doublet charge pair are investigated by Monte Carlo calculations in the SU(2) lattice gauge theory with a Higgs-scalar doublet. The mass ratio m_W/m_H and the shape of the static potential are used to obtain information on the renormalization group trajectories in the three-dimensional coupling constant space. Numerical evidence shows that only two of the couplings are relevant. The phase transition line on the border of the Higgs-phase is weakly first order. A lower bound $m_H/m_W \geq 1.0 \pm 0.3$ is obtained for the ratio of the Higgs-boson mass to the W-boson mass.

I. Introduction

In the standard SU(3) ⊗ SU(2) ⊗ U(1) model the two non-abelian gauge symmetry factors play rather different roles. The local gauge symmetry corresponding to SU(3)-colour is unbroken, the SU(3)-colour charges are confined and the colour interaction is strong. The local SU(2) gauge symmetry, on the other hand, is broken by the expectation value of the Higgs-doublet field, the SU(2) charges are screened and the corresponding interaction is weak. Since the values of the coupling constants are changing ("running" or "sliding") according to the renormalization group [1], the meaning of strong and weak couplings have to be explained in more detail. The renormalization group invariant meaning of "strong interaction" is that the ratio of the SU(3) Λ-parameter to the hadron masses is of order 1. Still a bit more precisely, we have for SU(3)-colour

$$\left| \ln \left(\Lambda_{SU(3)} / M_{hadron} \right) \right| \leq O(1) \quad . \qquad (I.1)$$

This statement takes into account, for instance, the factors between different reasonable Λ-parameter definitions (Λ_{mom}, $\Lambda_{\overline{MS}}$, $\Lambda_{lattice}$ etc.). In contrast to Eq.(I.1), for the SU(2) Λ-parameter and the W-boson mass (m_W) experiments imply

$$\Lambda_{SU(2)} / m_W \cong 10^{-23} \quad . \qquad (I.2)$$

This number can be obtained from the value of the SU(2) coupling strength at, say, the W-mass and from the renormalization group equation assuming, for definiteness, 3 standard fermion families and a single Higgs-scalar doublet. Eq.(I.2) implies that the SU(2) coupling is getting, in principle, strong at an energy scale of about 10^{-12} eV. This has, however, no practical consequences because of the short range of the interaction due to the massive SU(2) gauge boson exchange.

The smallness of $\Lambda_{SU(2)}/m_W$ may seem "unnatural" or "unaesthetic" unless there is some good reason for it. In fact, in the framework of grand unification [2] the

SU(3) and SU(2) couplings become equal at some very high energy scale $M_{GU} \sim 10^{15} - 10^{17}$ GeV, and Eq.(I.2) is explained by a relation like

$$\ln \frac{\Lambda_{SU(2)}}{m_W} = c \ln \frac{M_{hadron}}{M_{GU}} , \qquad (I.3)$$

with some constant c of order unity. The theoretical consequence of Eq.(I.2) is that the SU(2) ⊗ U(1) electroweak interaction can be treated by perturbation theory. The impressive success of the perturbative approach culminated not very long ago in the discovery of W- and Z-bosons at precisely the predicted masses [3].

The only remaining source of uneasiness in the standard model is buried in the Higgs-sector incorporating the inherently non-perturbative phenomenon of spontaneous symmetry breaking. The main interest of the non-perturbative investigation of the electroweak theory lies, in fact, in the deeper understanding of the Higgs-mechanism [4], which renders the W- and Z-bosons, the leptons and quarks and the, upto now elusive, Higgs-boson a mass.

Strong weak-interactions. In the present paper the Higgs-sector of the standard SU(2) ⊗ U(1) electroweak theory is investigated by the non-perturbative numerical Monte Carlo method [5]. The calculation is performed in a coupling constant range, where Eq.(I.2) is not fulfilled. On the contrary, similarly to Eq.(I.1), we shall typically consider the case

$$\left| \ln \left(\Lambda_{SU(2)} / m_W \right) \right| \leq O(1), \qquad (I.4)$$

i.e. the values of coupling constants will correspond to a situation where the SU(2) weak-interaction is strong. The electromagnetic interaction will be neglected altogether (no U(1)-factor) and no fermions (leptons and quarks) will be considered. For a possibility, how to include these in the lattice action see Ref. [6].

The study of the standard SU(2) Higgs-sector in the situation corresponding to Eq.(I.4) is interesting from several point of views:

i.) it can reveal the existence of non-perturbative constraints in the electroweak theory. For instance, the number of independent renormalized couplings can be smaller than the number of bare couplings. A large body of evidence [7] has been collected to support the occurence of such a "parameter reduction" in the single-component ϕ^4-theory, where the renormalized coupling is probably always zero;

ii.) it is interesting to compare and to confront the behaviour of the totally broken SU(2) gauge interaction with unbroken SU(N) colour, studied upto now in most Monte Carlo investigations;

iii.) the gauge-Higgs system is theoretically interesting for his own sake, as a representative of a class of quantum field theories;

iv.) finally, there has been some speculations that weak interactions could perhapes become strong in the hundred GeV energy range [8]. This possibility seems to be improbable at present, but direct experimental evidence is still scarce at such high energies.

Previous Monte Carlo simulations of the SU(2) Higgs-system with scalar field in the fundamental (doublet) representation [9-12] concentrated mainly on the singularity structure in the coupling constant space. These studies showed, that there is a phase transition surface separating the Higgs-phase from the confinement phase. These "phases" are, however, not qualitatively different from each other [13], they are continuously connected beyond the edge of the critical surface. This structure is illustrated by Fig. 1, which is a reproduction of Fig. 3 of the paper by Kühnelt, Lang and Vones [10].

An interesting question is the order of the phase transition separating the Higgs-like and confinement-like regions. If there is a critical surface corresponding to a second order phase transition, then the correlation length becomes infinite and some continuum theory can be defined in a limit going to this surface. (The continuum theory may be trivial, i.e. non-interacting, except perhapes for some peculiar "fixed points" on this surface.) Information on the critical behaviour can be obtained e.g. from "finite size scaling" [11] or from a direct study of the correlations [12].

In my previous paper [12] the correlations were numerically calculated in the limit of infinite self-coupling ($\lambda \to \infty$; fixed length Higgs-field on the

lattice). This limit of the standard electroweak theory was considered extensively in the literature [14] as an interesting limiting case, when the tree-level mass of the physical Higgs-boson tends to infinity. (The physical mass can, however, stay finite [15].) The results in Ref. [12] showed, that the correlation lengths in both the isovector 1^{--} (W-boson) and isoscalar 0^{++} (Higgs-boson) channels have a tendency to grow in the vicinity of the critical line. This could be interpreted as a sign for a second order phase transition, but a weakly first order transition with some small specific heat was equally possible. The present paper is an extension of Ref. [12] : in the case of fixed-length Higgs-field ($\lambda \to \infty$) more statistics is collected closer to the critical line and the variable length case is considered, too, for several values of the self-coupling λ . The precise position of the phase transition is determined in several points directly from the correlations and evidence is presented for a weakly first order transition for all λ -values. The correlations are determined also in another important limit, namely for $\beta \to \infty$ (no gauge coupling) [16]. Special emphasis is given to the information which can be obtained from the mass ratios and from the static potential concerning the renormalization group properties of the model.

In the next Section, after summarizing the lattice formulation of the SU(2) fundamental Higgs-model, the results for the correlations will be presented and discussed. The position and order of the phase transition will be determined. In Section III. the static energy of an external SU(2) doublet charge pair is considered and consequences for the renormalization group trajectories ("lines of constant physics") in the three-dimensional coupling constant space will be discussed. The last Section contains the conclusions.

II. Correlations

The lattice action. The continuum euclidean action S_c of an SU(2) gauge field interacting with a complex scalar doublet $\phi(x)$ can be written like

$$S_c = \int d^4x \left\{ \frac{1}{2} \mathrm{Tr}\left(F(x)_{\mu\nu} F(x)_{\mu\nu} \right) + \phi^+(x) \overleftarrow{D}_\mu \overrightarrow{D}_\mu \phi(x) + \lambda_c \left(\phi^+(x)\phi(x) - v^2 \right)^2 \right\} . \qquad \text{(II.1)}$$

Here $F(x)_{\mu\nu}$ denotes, as usual, the field-strength matrix of the gauge field, D_μ is the gauge-covariant derivative, λ_c is the self-coupling constant of the Higgs-field and v is the tree-level vacuum expectation value related to the opposite-sign mass term $-\mu^2 \phi^+(x)\phi(x)$ by

$$v = \frac{\mu\sqrt{2}}{\sqrt{\lambda_c}} . \qquad \text{(II.2)}$$

The gauge field is described on the lattice by the link variables $U(x,\mu) \in SU(2)$ and the Wilson gauge lattice action is a sum $\sum_P$ over positive orientation plaquettes P. For the lattice description of the Higgs-field it is convenient to introduce the lattice site variable ϕ_x and the lattice bare couplings $\varkappa, \lambda$ by the replacements

$$\begin{aligned} a\phi(ax) &\longrightarrow \sqrt{2\varkappa}\,\phi_x \\ \lambda_c &\longrightarrow \lambda \varkappa^{-2} \\ 8 - (a\mu)^2 &\longrightarrow (1-2\lambda)/\varkappa \end{aligned} \qquad \text{(II.3)}$$

Here a denotes, as usual, the lattice spacing. In these variables the euclidean lattice action is

$$S = \sum_x \left\{ \lambda (\phi_x^+ \phi_x - 1)^2 + \phi_x^+ \phi_x - \varkappa \sum_\mu \phi^+_{x+\hat{\mu}} U(x,\mu) \phi_x \right\} + \beta \sum_P \left\{ 1 - \frac{1}{2} \mathrm{Tr} U_P \right\} . \qquad \text{(II.4)}$$

The lattice is assumed to be periodic in all four directions. $\sum_x$ means a summation over all lattice sites, $\sum_\mu$ is a sum over positive and negative directions ($\mu = \pm 1, \pm 2, \pm 3, \pm 4$), $\hat{\mu}$ stands for a unit vector in direction μ and β is related to the bare gauge coupling g by $\beta = 4/g^2$.

The peculiarity of the SU(2) doublet field ϕ_x is that it can also be represented by its length $\rho_x \geq 0$ and by an SU(2) matrix α_x . The correspondence is given by ($\alpha = 1,2$):

$$\phi_x^\alpha = \rho_x \alpha_{x,\alpha 2} \quad ,$$
$$\tilde{\phi}_x^\alpha = \varepsilon_{\alpha\beta} \phi_\beta^+ = \rho_x \alpha_{x,\alpha 1} \quad . \qquad \text{(II.5)}$$

Here $\tilde{\phi}$ is the opposite hypercharge doublet field in SU(2) $\otimes$ U(1) (ε is the antisymmetric unit tensor). Using the new variables, the lattice action can be written as

$$S = \sum_x \left\{ \rho_x^2 - 3h\rho_x + \lambda(\rho_x^2 - 1)^2 - \kappa \sum_{\mu>0} \rho_{x+\hat{\mu}} \rho_x \mathrm{Tr}\left[\alpha^+_{x+\hat{\mu}} U(x,\mu) \alpha_x\right]\right\}$$
$$+ \beta \sum_p \left(1 - \frac{1}{2}\mathrm{Tr}\, U_p\right) \quad . \qquad \text{(II.6)}$$

The integration measure was originally $\rho_x^3 d\rho_x d^3\alpha_x d^3 U(x,\mu)$ (if $d^3 g$ denotes the invariant Haar-measure in SU(2)), but in Eq.(II.6) the factor ρ_x^3 is included in the exponent, therefore the measure is simply $d\rho_x d^3\alpha_x dU(x,\mu)$. Let us introduce, instead of the SU(2) link- and site-variables $U(x,\mu)$ and α_x , the gauge invariant link variable

$$V(x,\mu) \equiv \alpha^+_{x+\hat{\mu}} U(x,\mu) \alpha_x \quad . \qquad \text{(II.7)}$$

Due to local gauge invariance, this can be used for the description of the gauge field also in the pure gauge part, therefore the lattice action can be written like

$$S = \sum_x \left\{ \rho_x^2 - 3h\rho_x + \lambda(\rho_x^2 - 1)^2 - \kappa \sum_{\mu>0} \rho_{x+\hat{\mu}} \rho_x \mathrm{Tr}\, V(x,\mu)\right\}$$
$$+ \beta \sum_p \left(1 - \frac{1}{2}\mathrm{Tr}\, V_p\right) \quad . \qquad \text{(II.8)}$$

This does not depend on α_x , therefore the integration $d^3\alpha_x$ gives only an unessential constant factor and can be omitted. The integration measure for

Eq.(II.8) is $d\rho_x d^3 V(x,\mu)$. The disappearance of the angular part α_x of the Higgs-field is usually expressed by saying that it is"eaten" by the gauge field. Since both ρ_x and $V(x,\mu)$ are gauge invariant, both of them describe physical degrees of freedom: $V(x,\mu)$ corresponds to the (gauge-) W-boson and ρ_x to the physical (Higgs-) H-boson.

The SU(2) Higgs-model with Higgs-field in the fundamental representation has a global SU(2) "weak-isospin" symmetry. In the full SU(2) $\otimes$ U(1) electroweak theory this symmetry corresponds to the transformations $l \leftrightarrow \nu_l$ $(l = e, \mu, \tau)$, $u \leftrightarrow d$, $c \leftrightarrow s$, $t \leftrightarrow b$, therefore it is broken by electromagnetism and by fermion mass differences within doublets. In the action (II.8) the exact global weak-isospin symmetry transformation is

$$V'(x,\mu) = U^{-1} V(x,\mu) U \quad ; \quad \rho_x' = \rho_x \quad . \qquad \text{(II.9)}$$

For comparison, the local gauge transformation is

$$U'(x,\mu) = U_x^{-1} U(x,\mu) U_x \quad ,$$
$$\alpha_x' = U_x^{-1} \alpha_x \quad , \qquad \alpha_x^{+\prime} = \alpha_x^+ U_x \quad , \qquad \text{(II.10)}$$
$$V'(x,\mu) = V(x,\mu) \quad .$$

With respect to weak-isospin the W-boson is isovector, the Higgs-boson is isoscalar.

There are interesting limits of the model, which can be studied separately. In the case of infinitely strong self-coupling $\lambda \to \infty$ the length of the Higgs-field is frozen to $\rho_x = 1$, and the action is

$$S_{\lambda=\infty} = -\kappa \sum_{x,\mu>0} \mathrm{Tr}\, V(x,\mu) + \beta \sum_p \left(1 - \frac{1}{2}\mathrm{Tr}\, V_p\right) \quad . \qquad \text{(II.11)}$$

The correlations in this limit were investigated in Ref. [12]. This is the limit of a very strongly interacting Higgs-field, where μ and λ_c in Eq.(II.2)

go to infinity in such a way that the tree-level vacuum expectation value $v \cong a^{-1}\sqrt{\kappa}$ remains constant. The tree-level mass $\mu\sqrt{2}$ of the physical Higgs-boson goes also to infinity. Nevertheless, as it was shown in Ref. [12] and as we shall see below in more detail, the lowest mass in the isoscalar 0^{++} channel remains finite.

Another important limit of the action in Eq.(II.8) is $\beta \to \infty$ (zero gauge coupling). In this case the link variable $V(x,\mu)$ is a pure gauge, therefore it is more convenient to restore the angular Higgs-variable α_x and return to Eq.(II.6), which gives

$$S_{\beta=\infty} = \sum_x \{\rho_x^2 - 3\ln\rho_x + \lambda(\rho_x^2-1)^2 - \kappa \sum_{\mu>0} \rho_{x+\hat{\mu}}\,\rho_x\, \mathrm{Tr}(\alpha^+_{x+\hat{\mu}}\,\alpha_x)\}. \quad \text{(II.12)}$$

This is the lattice version [16] of the Gell-Mann-Lévy linear σ-model [17]. It has a global SU(2) $\otimes$ SU(2) symmetry corresponding to the transformation ($U_\pm \in SU(2)$):

$$\alpha'_x = U_-^{-1}\,\alpha_x\,U_+ \quad . \quad \text{(II.13)}$$

SU(2) $\otimes$ SU(2) is equivalent to O(4) and the SU(2) group elements can also be represented by a unit-length four-vector (a_0, a_τ):

$$\alpha_x = a_{0,x} + i\tau_\tau a_{\tau,x} \quad (\tau_\tau = \text{Pauli-matrix}) \quad \text{(II.14)}$$

In the limit $\lambda \to \infty$ the model in Eq.(II.12) becomes the non-linear O(4) σ-model in four dimensions:

$$S_{\beta=\infty,\lambda=\infty} = -2\kappa \sum_{x,\mu>0} a_{\rho,x+\hat{\mu}}\; a_{\rho x} \quad . \quad \text{(II.15)}$$

In the continuum limit the action $S_{\beta=\infty}$ in Eq.(II.12) is expected to describe 3 massless Goldstone-bosons and 1 massive scalar particle, which are presumably non-interacting [18].

Monte Carlo calculation of the correlations. The Monte Carlo simulation in the SU(2) fundamental Higgs-model can be done by using the lattice action in Eq.(II.8). For the fixed length case ($\lambda \to \infty$) the action is given by (II.11). In the present paper the correlations were computed on an 8^4 lattice. The SU(2) link variables were replaced in most cases by the elements of the 120-dimensional icosahedral subgroup. The updating was done by the Metropolis-method with 6 hits per link for the gauge field $U(x,\mu)$ and 6 hits per site for the length variable ρ_x. The links and sites were updated in a random order, but always full sweeps were performed alternating over links and sites.

Diagonal correlations (and sometimes a few off-diagonal ones) were measured in different channels. In all cases the three-momentum was projected out both to $\underset{\sim}{p}=0$ and $\underset{\sim}{p}=\pi/(4a)$ (1 in lattice units) in all three space-like directions. The time-slices were chosen in all four possible orientations. The measurement of the correlations was performed only after every 5^{th} or 10^{th} full sweep in order to reach more independent configurations. The results given below were collected typically from 8000-10000 sweeps for every point in the coupling constant space. The configuration was started in most cases from a previously equilibrated configuration in some neighbouring point. At least 1000 equilibrating sweeps were performed before starting to collect data on the correlations. The computer time used for the calculation of correlations amounted to about 400 CPU hours on the Siemens 7.882 at the University of Hamburg.

To obtain the correlations in the W-boson channel an appropriate operator is

$$O^{(m)}_{W\tau} = \mathrm{Tr}\left[\tau_\tau V(x,m)\right] \qquad (m,\tau = 1,2,3). \quad \text{(II.16)}$$

As it was discussed in Ref. [12], this has weak-isospin $I_W=1$ and spin-parity $J^{PC}=1^{--}$. For the $I_W=0$ Higgs-boson channel there are several possibilities:

$$O_G = \sum_{(m,n)} \mathrm{Tr}\, V_{p(m,n)} \quad , \qquad O_H = \rho_x \quad , \qquad O_A = \sum_m \mathrm{Tr}\, V(x,m) \quad . \quad \text{(II.17)}$$

The first is the symmetric combination of the three space-like orientation single plaquette operators, which is often used in QCD glueball spectrum calculations for the 0^{++} channel. The second is the genuine $I_W=0$, $J^{PC}=0^{++}$ Higgs-variable (the length of the Higgs-field). The third operator appears in the $\lambda=\infty$ action (II.11). Assuming that the 0^{++} state is the lowest isoscalar state, the symmetrization in O_G and O_A can also be omitted, provided that the correlation is determined at large enough distances and therefore the higher mass contributions from othe spin-parity channels can be neglected. Similarly, the lowest mass can also be inferred from off-diagonal correlations, like e.g. between $\mathrm{Tr}V(x,m)$ and $\mathrm{Tr}V(x,n)$ $(m\neq n)$, if the distance is large enough.

The results obtained for the correlations in the W- and H-boson channels are shown in Figs. 2A-2C and in Table I. Always the inverse correlation lengths are given, i.e. the estimate of the lowest mass in lattice units in the given channel. Table I also contains some global average quantities like the average link L, average plaquette P, average length ρ, length dispersion σ_ρ and average action per site s. These are defined, respectively, like

$$L=\left\langle\frac{1}{2}\mathrm{Tr}V(x,\mu)\right\rangle,$$

$$P=\left\langle 1-\frac{1}{2}\mathrm{Tr}V_p\right\rangle,$$

$$\rho=\langle\rho_x\rangle,\qquad \sigma_\rho=\sqrt{\langle\rho_x^2\rangle-\langle\rho_x\rangle^2},$$

$$s=6\beta\left\langle 1-\frac{1}{2}\mathrm{Tr}V_p\right\rangle+\left\langle\rho_x^2-3h\rho_x+\lambda(\rho_x^2-1)^2\right\rangle+ \tag{II.18}$$

$$+8\varkappa\left\langle 1-\frac{1}{2}\rho_x\rho_{x+\hat\mu}\,\mathrm{Tr}V(x,\mu)\right\rangle.$$

In the average action per site the constant term $8\varkappa$ is added with respect to Eq.(II.8), in analogy to the constant 6β in the average plaquette term.

In the W-boson channel, for $am_W\lesssim 1$, the correlation can be determined, with relatively small errors, upto the maximum distance $d=4$ on the 8^4 lattice.

The correlations in some sample points were shown in Ref. [12]. The qualitative behaviour is here rather similar. The easiness of the measurement of correlations at larger distances reminds the general behaviour in 2-dimensional σ-models [19] and not the pure SU(2) gauge theory, where it is rather difficult to obtain large distance correlations [20]. For $am_W\gtrsim 1.5$ the correlation drops fast at small distances. In such points the mass estimate is obtained from distance $d=1$ (or at most from $d=2$), therefore these points have large systematic errors. The errors shown include some subjective estimate of the systematic errors, too.

In the case of the Higgs-boson channel the situation is more involved. The one-plaquette operator O_G in Eq.(II.17) behaves rather similarly, or even still somewhat worse, than in pure SU(2) gauge theory, i.e. the correlation usually cannot be determined beyond $d=1$. The best points for O_G are below the phase transition line ($\varkappa<\varkappa_{cr}$, see below), where the behaviour, and also the value of the correlation length, is rather similar to pure SU(2) gauge theory at the same β-value [20]. The other two operators O_H and O_A behave oppositely: for $\varkappa<\varkappa_{cr}$ they are worse, for $\varkappa>\varkappa_{cr}$ however much better than O_G. For $\varkappa>\varkappa_{cr}$ the diagonal correlation of O_H and O_A can be determined, within the given statistics, upto $d=2$ or $d=3$. O_A behaves for $\lambda>0.1$ still somewhat better than O_H, but the mass estimates from O_A and O_H are always compatible. In the Figures and in Table I always the best estimate for am_H is given, sometimes including also information from the off-diagonal correlations between $\mathrm{Tr}V(x,m)$ and $\mathrm{Tr}V(x,n)$ $(m\neq n)$.

The energies E_1 obtained from the $\vec{p}=1$ correlations give in most cases, within errors, the same mass $m=\sqrt{E_1^2-\vec{p}^2}$ as the $\vec{p}=0$ time-slices. This shows that Lorentz-invariance is approximately restored in the measured points. There seem to exist, however, some systematic deviations in the points with largest correlation lengths ($\xi\gtrsim 2$), where the $\vec{p}=1$ mass is usually 1o-2o% higher. This may be due to finite size effects, since finite cut-off effects are expected to become smaller for large ξ.

Behaviour near the phase transition. The qualitative behaviour of am_W and am_H for $\beta=2.3$, $\lambda=\infty$ (Fig. 2A), $\beta=2.3$, $\lambda=1.0$ (Fig. 2B) and $\beta=2.3$, $\lambda=0.1$ (Fig. 2C) is quite similar. The main difference is in the widths of the $\varkappa$-

range, where similar changes occur: the region near the phase transition is squeezed for small λ . The reason of this behaviour is quite clear: at $\lambda=0$ the model defined by the action (II.8) has a kinematical singularity. In the Higgs-phase, where the link expectation value is substantial ($L\to 1$ for $\varkappa\to\infty$), for large enough "hopping parameter" $\varkappa$, the hopping term proportional to $\varkappa$ wins over the stabilizing ρ_x^2 term and the action is unbounded from below if $\rho_x\to\infty$. For very small λ the $\lambda(\rho_x^2-1)^2$ term can stabilize the theory only for very large ρ_x , therefore the change above $\varkappa_{cr}$ is squeezed into a small $\varkappa$ -region, which is asymptotically proportional to $\sqrt{\lambda}$.

Appart from the squeezing, there is a remarkable universal behaviour for different λ . This can already be seen in the global averages given in Table I. For instance, the link expectation value is a universal function of the plaquette expectation value (see Fig. 3). This shows, that $\varkappa$ is not the correct variable to use. Plotting the W-boson mass as a function of the link expectation value, one obtains the remarkable universal curve shown in Fig. 4A. The same for the Higgs-boson mass, in Fig. 4B, shows a universal behaviour,too, although the errors are larger and maybe there is some mild tendency for the $\lambda=0.1$ points to fall somewhat below the rest. Fig. 4B has to be contrasted, however, with the tree-level prediction $m_H=v\sqrt{\lambda_c}$, according to which m_H should go to infinity for $\lambda\to\infty$.

Figures 4A and 4B reveal a discontinuous behaviour of the masses at $L=L_{cr}\cong 0.26$. At this point am_W jumps from values around $am_W\sim 0.5$ to $am_W\gtrsim 2.0$. At the same time am_H jumps from $am_H\sim 0.5$ to $am_H\sim 1.2$, a value consistent with the 0^{++} glueball mass at the same β in SU(2) [20]. Therefore, at $\beta=2.3$ the critical surface on the border of the Higgs-phase is discontinuous (first order) for all λ -values considered. This is not really in contradiction with Refs. [9-10], where the phase transition was classified as second order, because the hysteresis associated with the transition is rather weak. Some two-state jump behaviour in the updating can only be seen for the smallest λ value ($\lambda=0.1$). The position of the weakly first order transition is, however, substantially lower than the lines given in Ref. [19] and shown also in Fig. 1. The present best estimates for $\varkappa_{cr}$ are (always for $\beta=2.3$):

$$\begin{aligned}
\lambda=\infty: &\quad \varkappa_{cr}=0.386\pm 0.005 \\
&\quad \Delta\varkappa\cong 0.3 \\
\lambda=1.0: &\quad \varkappa_{cr}=0.303\pm 0.002 \\
&\quad \Delta\varkappa\cong 0.09 \\
\lambda=0.1: &\quad \varkappa_{cr}=0.192\pm 0.001 \\
&\quad \Delta\varkappa\cong 0.02
\end{aligned} \qquad \text{(II.19)}$$

The $\Delta\varkappa$ values give the approximate widths of the typical structure above $\varkappa=\varkappa_{cr}$ (for $\lambda\to 0$ $\Delta\varkappa$ is expected to vanish like $\sqrt{\lambda}$). Concerning the order of the phase transition, the Aachen-group reported very recently some preliminary evidence in favour of a two-state structure at very small λ values [21].

An interesting observation at the phase transition is, that the average action per point S has a maximum at $\varkappa=\varkappa_{cr}$ (see Fig. 5). The instability associated to this maximum is an intuitive reason why the phase transition is discontinuous. Let us note, that the perturbation-theoretic Coleman-Weinberg phenomenon [22-23] also implies a first order transition.

Below the phase transition ($\varkappa<\varkappa_{cr}$) everything looks very much like in pure SU(2) gauge theory (further arguments in this direction will be given in the next Section). In the Higgs-phase ($\varkappa>\varkappa_{cr}$), far away from the phase transition, m_H is roughly twice as large as m_W (this is similar to the situation in a Type I superconductor with $m_H>m_W$ [23]). Near the critical line, however, m_H and m_W becom nearly equal. Due to the somewhat large errors it is impossible at present to say, whether there is a region for $\varkappa>\varkappa_{cr}$ also with $m_H<m_W$ (like in Type II superconductors). For the moment the numbers are consistent with $m_H\geq m_W$ (with error: $m_H\geq(1.0\pm 0.3)m_W$), but further Monte Carlo studies on larger lattices and higher statistics can decide whether $m_H<m_W$ is possible or not. The lower bound for the Higgs-boson mass $m_H\geq(1.0\pm 0.3)m_W$ is relevant (upto electromagnetic and fermionic corrections) also to the real world with small gauge coupling, since m_H/m_W increases for decreasing gauge coupling strength (see the next Section in connection with the discussion of the renormalization group trajectories).

Let us note, that concerning the occurence of $m_H\cong m_W$ the present conclusions

differ somewhat from those of Ref. [12]. The reason is the better statistics closer to the phase transition, which allowed a more precise localization of the phase transition. Points with $m_H \cong m_W$ were found in Ref. [12] only near the endpoint of the phase transition line (near $\beta=1.5$). Here we see that such points occur also at $\beta=2.3$ (and very probably also for every larger β), if one is going close enough (from above) to $\varkappa=\varkappa_{cr}$.

Correlations at $\beta=\infty$. The $\beta\to\infty$ limit of the correlations can be numerically studied by a separate Monte Carlo simulation based on the action in Eq.(II.12). This is equivalent to an O(4) σ-model in 4 dimensions, therefore the O(4) variables defined in (II.14) can also be used. For technical reasons, however, I took the SU(2) $\otimes$ SU(2) action (II.12) and used for the SU(2) site variables (α_x) the elements of the icosahedral subgroup.

Let us denote the inverse correlation length at $\beta=\infty$ measured by the Higgs-field length variable ρ_x by am_h. For the inverse correlation length between the angular variables α_x let us introduce the notation am_g . In the continuum limit discussed below m_h is the mass of the massive Higgs-boson, whereas m_g is the mass of the 3 Goldstone-bosons. We expect, namely, at some critical value $\varkappa=\varkappa_{cr}$ (which is a function of λ : $\varkappa_{cr}=\varkappa_{cr}(\lambda)$) spontaneous symmetry breaking. On the lattice this is manifested for $\varkappa\geq\varkappa_{cr}(\lambda)$ by a spontaneous alignment of the SU(2) variables in some arbitrary direction. The consequence of the spontaneous symmetry breaking SU(2) $\otimes$ SU(2) $\longrightarrow$ SU(2) (or equivalently O(4) $\longrightarrow$ O(3)) is the appearance of 3 massless Goldstone-bosons ($m_g=0$) in the continuum limit.

The Monte Carlo simulation at $\beta=\infty$ was carried out, similarly to the $\beta<\infty$ case, on an 8^4 lattice. In the Metropolis updating procedure the site variables α_x and ρ_x were updated simultaneously, with 6 hits per site (in a randomly chosen order of sites). Concerning the number of sweeps and the amount of statistics the same applies as for the finite β simulation (see above). The results obtained for am_g and am_h are shown in Figs. 6A and 6B and in Table II. In the Table the average link L , the average length ρ , the length dispersion σ_ρ and average action per site s are also included. These are defined, similarly to (II.18), like

$$L=\left\langle \frac{1}{2}\,\mathrm{Tr}\left(\alpha^{+}_{x+\hat{\mu}}\,\alpha_x\right)\right\rangle ,$$

$$\rho=\langle\rho_x\rangle , \qquad \sigma_\rho=\sqrt{\langle\rho_x^2\rangle-\langle\rho_x\rangle^2} ,$$

$$s=\left\langle \rho_x^2-3\ln\rho_x+\lambda(\rho_x^2-1)^2\right\rangle+8\varkappa\left\langle 1-\frac{1}{2}\,\rho_x\rho_{x+\hat{\mu}}\,\mathrm{Tr}\left(\alpha^{+}_{x+\hat{\mu}}\,\alpha_x\right)\right\rangle . \qquad \text{(II.20)}$$

As a function of the average link L , there is a similar universality as for finite β (see Fig. 7).

As it is shown by Fig. 7, at the critical link expectation value $L=L_{cr}\cong 0.2$, spontaneous symmetry breaking takes place. Above this critical point the Goldstone-boson mass (in lattice units) am_g is consistent with zero. At $L=L_{cr}$ the Higgs-mass (in lattice units) am_h has a minimum value of $am_h=0.4\pm0.1$. The critical $\varkappa$ at the two λ-values is, respectively:

$$\lambda=1.0: \qquad \varkappa_{cr}=0.247\pm0.003$$

$$\lambda=0.1: \qquad \varkappa_{cr}=0.164\pm0.001 \qquad \text{(II.21)}$$

The inverse correlation lengths around the critical point behave continuously (there is no discontinuity like in Fig. 4A-4B). This is consistent with the expected second order phase transition. Above the critical point there are very long range correlations in the angular variables, extending practically over the whole lattice. In fact, the value of the angular correlation is typically only 5-10% smaller between the most distant (d=4) time slices than for d=1. In the limit $\varkappa\to\varkappa_{cr}$ the asymptotic behaviour of the correlations in the angular variables is expected to be power-like (it goes to zero like the inverse of the euclidean distance to the power $(2+\eta)$ where η is some critical exponent [7]). It is remarkable, that the measured correlation length for the length variable in the broken symmetry phase $\varkappa>\varkappa_{cr}$ is quite different from zero. This would not be the case for a strong coupling of the Goldstone-modes to the Higgs-particle, since for sufficiently strong coupling the two-Goldstone-boson cut at zero mass would dominate. The small coupling is consistent with

the expectation that the SU(2) doublet ϕ^4-theory has a non-interacting continuum limit for $\varkappa \to \varkappa_{cr}(\lambda)$ (λ fixed).

It will be argued in the next Section, that the continuum limit in the coupled gauge-Higgs system is $\beta \to \infty$ and $\varkappa \to \varkappa_{cr}(\lambda)$ (from above in the Higgs-phase) for any non-zero λ. Let us note, that according to Fig. 7, for $\beta = \infty$ (exactly zero gauge coupling) and $\varkappa \to \varkappa_{cr}(\lambda)$ the correlation length in the Higgs-field length remains finite in lattice units. Therefore, the $\beta \to \infty$ limit of the Higgs-mass in the gauge-Higgs system $\lim_{\beta\to\infty} a m_H = 0$ is not equal to $a m_h > 0$ measured at $\beta = \infty$. The pure Higgs-field length fluctuations remain infinitely short range compared to the fluctuations in the interacting theory. Another aspect of $a m_h > 0$ is, that in the continuum limit $\varkappa \to \varkappa_{cr}(\lambda)$ (λ fixed) of the pure Higgs-system the mass corresponding to the Higgs-field length is infinite, therefore the model describes only three non-interacting zero-mass scalar particles.

III. Static energies

Wilson-loops. The static energy $E(R)$ of an external SU(2)-doublet charge pair is a characteristic property of the SU(2) gauge-field system: in the case of confinement it increases linearly for large distances, whereas in a screening phase (like the Higgs-phase) it goes asymptotically to a constant. As it is well known, $E(R)$ can be determined from the expectation value of Wilson-loops $W_{R,T} \equiv \frac{1}{2} \mathrm{Tr} U_{R,T}$ with time elongation T and euclidean distance R between the endpoints for fixed time:

$$a E(R) = - \lim_{T\to\infty} \frac{1}{T} \ln W_{R,T} \quad . \qquad \text{(III.1)}$$

Some Monte Carlo measurements of the static energy $E(R)$ were performed on 8^4 lattice in Ref. [12], where it was shown that rotation invariance of $E(R)$ is well satisfied if the largest correlation length is at least 1.

In this paper a more detailed study of the static energies will be presented.

It was carried out on 12^4 lattice using the icosahedral subgroup for the SU(2) variables. The lattice actions (II.8) and (II.11) were used, and the Wilson-loops were calculated from the gauge invariant links $V(x,\mu)$. This is equivalent, because of gauge invariance, to the use of the original link variables which appear in the definition of $W_{R,T}$. The values of planar Wilson-loops with $1 \le R, T \le 5$ were determined (after ~ 1000 equilibrating sweeps) in 2000-3000 sweeps for some selected points in the 3-dimensional parameter space ($\lambda, \beta, \varkappa$). The results are collected in Tables IIIA-IIIC. This calculation took about 600 CPU hours on the Siemens 7.882 computer at the University of Hamburg.

Because of the limitation in time elongation T, the best way to extract the static energy $E(R)$ is to fit the 5 points ($1 \le T \le 5$) by the sum of two exponentials:

$$W_{R,T} = c_{1R} e^{-\varepsilon_{1R} T} + c_{2R} e^{-\varepsilon_{2R} T} \quad . \qquad \text{(III.2)}$$

The industrious reader is invited to repeat the calculation on the basis of Table III. Here only the final results will be shortly summarized: the fit is good and the value of the smaller energy ε_{1R} is always stable with small error. Therefore, one can identify $a E(R)$ with ε_{1R}. The second energy ε_{2R} is also reasonably well determined, and its value is typically 3-6 times larger than ε_{1R} (typical values of ε_{2R} are in the range 1.6-2.3). This means that the field configuration around the external charge pair is sufficiently rigid and the static energy can be considered, to a good approximation, as a potential energy.

The R-dependence of the potential for $1 \le R \le 5$ was compared to 3 simple forms:

$$a E(R) = \begin{cases} -\frac{\alpha}{R} e^{-amR} + c & \text{(Yukawa)} \\ -\frac{\alpha\, am}{(e^{amR} - 1)} + c & \text{(Hulthén)} \\ -\frac{\alpha}{R} + a^2 \sigma R + c & \text{(string)} \end{cases} \qquad \text{(III.3)}$$

The best fit parameters are given in Table IV in those cases, when an accept-

able fit could be obtained by the given form. The systematic errors of the fitting procedure were roughly estimated from the deviations in such cases, when different fits were possible.

As it can be seen from Table IV, the Yukawa- or Hulthén-form gives a good fit in the Higgs-phase far enough from the phase transition surface. Therefore, the potential in these points is given, to a good approximation, by the massive W-boson exchange. For typical examples see Fig. 8. The fitted mass values am in Table IV are, within errors, consistent with the W-boson mass am_W determined from the correlations (see Table I). There is, however, some systematic difference between the Yukawa- and Hulthén-form: the former gives always smaller masses than the latter. Approaching the phase transition surface from above, the potential develops a quasi-linear, confinement-like behaviour for intermediate distances. The change between the pure Yukawa-like and more and more explicit string-like behaviour is continuous (for illustration see Fig. 9). Near the phase transition the Yukawa-fit gets gradually worse (see e.g. Figs. 10A-10B). It is expected, that in the Higgs-phase at very large distances the potential finally tends always to a constant, but the turn-over might set in rather late. Eventually, it would be very interesting to know the exact behaviour at very large R. For instance, if the $R\to\infty$ form is given by $const. - \frac{\omega}{R}\exp(-am_W R)$, then the value of ω could be quite different (e.g. much smaller) than the short distance coupling α. Further Monte Carlo studies may give some hints in this direction, but this is presumably a rather difficult question for a numerical study. Below the phase transition surface the potential becomes rather similar to the pure gauge theory confinement potential. For instance, at ($\lambda=\infty, \beta=2.3, \varkappa=0.3$) there is almost no difference compared to $\beta=2.3$ in pure SU(2) gauge theory (see Tables III-IV and Fig. 11).

Concerning the λ-dependence of the potential, if the average link L is used as variable (like e.g. in Figs. 4A-4B), then the same universal behaviour is observed as in the correlation lengths. For fixed λ the pattern of the short distance behaviour of the potential can be characterized by the "renormalized gauge coupling" α obtained in the fits (III.3). This definition of the renormalized coupling is, of course, not very precise, because strictly speaking α is a function of R. But for a first qualitative understanding it

is sufficient to consider the average defined by the fits. Taking the $\lambda=\infty$ values of α from Table IV, a simple linear interpolation gives the curves of constant coupling shown in Fig. 12.

"Chiral" loops. The potential energies deduced from Wilson-loops refer to a pair of infinitely heavy particles, which are transforming as a vector-like (i.e. non-chiral) doublet under SU(2). In the SU(2) $\otimes$ U(1) electroweak theory the fermions (leptons and quarks) are in a chiral representation: left-handed fermions form doublets, but the right-handed ones are scalars. The chiral transformation property can influence the forces acting on a heavy particle. In order to have a feeling on this effect, let us consider heavy, chiral, naive fermions on the lattice. The fermion matrix in the bilinear fermion action can be written, in this case, like

$$Q = 1 - K\sum_{\mu}\left\{\frac{1-\gamma_5}{2}\gamma_\mu V(x,\mu) + \frac{1+\gamma_5}{2}\gamma_\mu\right\} . \qquad \text{(III.4)}$$

Here $V(x,\mu)$ is the gauge invariant link variable introduced in the previous Section and K is the hopping parameter inversely proportional to the mass. In the hopping parameter expansion, for very heavy fermions, only the shortest paths contribute. (For a review of the hopping parameter expansion see [24].) This gives the straight time-like sides of the Wilson-loops for non-chiral fermions. In the case of (III.4) the dominant contribution for $K\to 0$ is again the straight line, but instead of a product of all link variables along the time-like sides, we have the product of every second (gauge invariant) $V(x,\mu)$. For the space-like sides, representing the field between external charges, it is possible to take both a full product of all links or every second link (or even more complicated products of links). For the simplicity of comparison, let us take full products. In Fig. 13 the potential extracted from such "chiral" loops is compared to the potential obtained in the same way from Wilson-loops at ($\lambda=\infty, \beta=2.3, \varkappa=0.5$). As it can be seen from the Figure, the potential energy is reduced somewhat at larger distances by the chiral transformation property, but the overall qualitative behaviour remains the same.

Difermion "zoo". The interesting consequence of the potential acting on a heavy fermion doublet pair is the possibility of bound states in difermion channels. (Note that the SU(2) representations are real, therefore both fermions and anti-fermions feel the same potential.) Even a pure Yukawa-potential $-\alpha \exp(-m r)/r$ has bound states, if the coupling α is large enough and if the constituents are heavy enough. A short numerical investigation shows, that the existence of at least one bound state in the non-relativistic Schrödinger-equation is guaranteed for $\alpha M/m$ (M is the reduced mass). The largest α value in Fig. 12 is around $\alpha \cong 1/3$, therefore $M/m_W > 3$ is enough. Of course, the quasi-confining potential shape near the phase transition line is even more favourable for bound states than the Yukawa-like potential.

In a world with strong "weak interactions" there would be many different kind of difermion bound states: SU(3) colour octets, sextets etc. from 2 quarks, lepto-quarks from a lepton and a quark, bound states of 2 leptons and so on. It is interesting, that states with similar quantum numbers were proposed recently in different contexts, in order to explain some strange kind of events seen at the proton-antiproton collider and at PETRA. From the long list of papers let us just mention Ref. [25], where colour-octet bound states were introduced, and Ref. [26], where lepto-quarks were proposed.

Assuming, that weak-interactions become somehow strong at a few hundred GeV, the explanation of such bound states would be rather easy, if there were a fourth standard fermion family with masses in the 1oo GeV range. The question remains, of course, open how weak interaction could be weak at low energy and strong at high energy. As a logical possibility, let us remind the above discussion about the short distance ($-\alpha/r$) and very long distance ($c - \omega \exp(-m_W r)/r$) behaviour of the potential in the Higgs-phase near the phase transition line. If ω were much smaller than α, the puzzle would be solved.

Renormalization group trajectories. An important question in the lattice-regularized SU(2) fundamental Higgs-model is, whether there exists a continuum limit defining a non-trivial (i.e. interacting) quantum field theory. The first complication compared to the pure gauge theory (where the existence

of a non-trivial continuum limit is generally assumed, but upto now is not mathematically proved) is the presence of several independent couplings. Therefore, let us first state in general terms how the continuum limit should look like in principle, if there are several independent couplings.

Let us consider a lattice field theory with n coupling constants $[g] \equiv g_1, g_2, \dots, g_n$. In order to define the "renormalization group trajectories" (RGT's) in the space of coupling constants let us choose a "reference quantity" m_1 with physical dimension of mass. Its value in lattice units $\mu_1 = a m_1$ is a function of the couplings: $\mu_1 = \mu_1[g]$. In addition, let us choose ($n-1$) independent, dimensionless ratios of physical quantities: $[\xi] \equiv \xi_2, \xi_3, \dots, \xi_n$, and consider the "curves of constant reference ratios" $C_{[\xi]}$ with $\xi_k = \text{const.}$ ($k = 2, \dots, n$). Along such curves the change of the reference quantity $\mu_1 = a m_1$ defines the change of the lattice unit a uniquely. An absolute value of a in terms of some units (e.g. eV^{-1}) is specified if the physical value of m_1 as a function of $[\xi]$ is given. A simple possibility is to take the value of m_1 $[\xi]$-independent, but other choices can be sometimes more advantageous. (One has to keep in mind, that for $m_1 = [\xi]$-independent the absolute scale on $C_{[\xi]}$ depends on the choice of the refence quantity m_1 .) On a given curve $C_{[\xi]}$ the coupling constants g_i $(i = 1, \dots, n)$ can be considered as functions of the lattice spacing: $g_i = g_i^{[\xi]}(a)$, and the corresponding β-function can be defined as

$$\beta_i[g] \equiv -a \frac{dg_i^{[\xi]}(a)}{da} \,. \qquad \text{(III.5)}$$

Sometimes it is also convenient to choose a reference coupling, say, g_1 and consider, on a given curve $C_{[\xi]}$, the lattice spacing and the other couplings as functions of it: $a = a^{[\xi]}(g_1)$ and $g_k = g_k^{[\xi]}(g_1)$ $(k = 2, 3, \dots, n)$. In this case one has, obviously

$$\frac{dg_k^{[\xi]}}{dg_1} = \frac{\beta_k[g]}{\beta_1[g]} \,. \qquad \text{(III.6)}$$

This can be considered as a differential equation for the curves of constant reference ratios.

The necessary condition for the existence of a continuum limit is, that there exists (at least one) "critical point" $[g_c] = g_{1c}, g_{2c}, \cdots, g_{nc}$ in the coupling space, such that

i.) $[g_c]$ lies on some subset $\mathcal{R}_c$ of the curves of constant reference ratios;

ii.) for $C_{[\mathcal{F}]} \in \mathcal{R}_c$ we have $\lim_{g_1 \to g_{1c}} a^{[\mathcal{F}]}(g_1) = 0$;

iii.) every (in general dimensionful) physical quatity $\mathcal{P}$ measured on the lattice tends on $C_{[\mathcal{F}]} \in \mathcal{R}_c$ for $[g] \to [g_c]$ to a $[\mathcal{F}]$-dependent value $\mathcal{P}_c^{[\mathcal{F}]}$ in such a way, that the deviation from the limiting value vanishes at least as fast as some power of μ_1 (or of a).

In other words, physical quantities are constant along $C_{[\mathcal{F}]} \in \mathcal{R}_c$ in the vicinity of the critical point $[g_c]$ upto corrections ("lattice artifacts") of order at most μ_1. It is useful to define a "scaling region" $\mathcal{S}_c$ belonging to $[g_c]$ by the requirement that the deviation of physical quantities from the continuum limit $\mathcal{P}_c^{[\mathcal{F}]}$ is in some specified sense "small" for $[g] \in \mathcal{S}_c$. Within the scaling region $\mathcal{S}_c$ the curves $C_{[\mathcal{F}]}$ can simply be called "curves of constant physics". Because of the above mentioned freedom in defining the scale, it is natural to consider the dimensionful physical quantities as functions of the lattice spacing a and of the couplings $[g]$: $\mathcal{P} = \mathcal{P}(a, g_1, \cdots, g_n)$. In the scaling region $\mathcal{S}_c$ the constancy of the physical quanties along the curves of constant physics can be expressed by the "renormalization group equation" (RGE):

$$\left\{ -a\frac{\partial}{\partial a} + \sum_{i=1}^{n} \beta_i[g] \frac{\partial}{\partial g_i} \right\} \mathcal{P} = O(\mu_1) \,. \qquad \text{(III.7)}$$

Here the right hand side stands for the "scaling violating" lattice artifacts. This equation reflects the fact, that in the scaling region the change in lattice spacing can be compensated (upto lattice artifacts) by an appropriate change ("renormalization") in the couplings. The curves of constant physics can also be called "renormalization group trajectories".

It can happen, that the limiting values $\mathcal{P}_c^{[\mathcal{F}]}$ of the physical quantities are the same for different curves $C_{[\mathcal{F}]}$. If the set of curves with equal limiting values spans out a hyperplane of dimension ℓ, one can say

that only $(n-\ell)$ couplings are "relevant" (ℓ couplings are irrelevant). In this case the irrelevant couplings can be omitted (or kept constant). The RGE will be valid with $(n-\ell)$ istead of n couplings. A critical point $[g_c]$ with $(n-\ell)$ relevant couplings can be said to have "rank" $(n-\ell)$.

In general there can be many (even an infinity) of critical points. It is also possible, that the above requirement iii.) is fulfilled only for some well defined subset $\mathcal{Q}_c$ of physical quantities. (For instance, $\mathcal{P} \in \mathcal{Q}_c$ is allowed to depend only on some subset of field variables.) Such a critical point can be called "reduced". The number of relevant couplings for a reduced critical point is usually smaller (its rank is lower), than for a normal critical point.

In order to see, how these notions work in a specific case, let us consider QCD with a single (dynamical) quark mass. In this case there are two couplings: the gauge coupling g (or $\beta = 6g^{-2}$) and the dimensionless quark mass variable μ_q (for Wilson-fermions one can define $\mu_q = (2K_q)^{-1}$, where K_q is the hopping parameter). The renormalization group trajectories are conventionally parametrized by the renormalization group invariant quark mass M_q (more precisely, by the ratio M_q/Λ, where Λ is the usual RG Λ-parameter for the SU(3) gauge coupling). The expected shape of the scaling region and of the RGT's $\mu_q = \mu_q(\beta)_{M_q}$ in the (β, μ_q)-plane are shown in Fig. 14. (For a more detailed discussion of QCD with dynamical quarks see Ref. [24].) The curve $\mu_{cr}(\beta)$ is the line with zero quark mass $M_q = 0$ ($\mu_{cr}(\beta)^{1\text{loop}}$ is its 1-loop perturbative approximation). The scaling region is, for $M_q \geq 0$, below the line (SQ). The critical point, where all the RT's with constant M_q meet, is at $(\beta = \infty, \mu_q = 4)$. If only pure gluonic quantities (like glueball mass, string tension etc.) are considered, the scaling region is larger: it is for $M_q \geq 0$ the whole region to the right of the line (SG). For this reduced set of physical quantities there is only one relevant coupling (for instance β), and there exists an infinity of reduced critical points along the line $\beta = \infty$, $4 < \mu_q \leq \infty$.

In the SU(2) fundamental Higgs-model the study of correlations and static energies gives valuable information on the RGT's. Along the RGT's the mass ratio m_H / m_W has to be constant, and the force $a^2 \, dE(\frac{r}{a}) / dr \equiv F(R)$

acting on the external doublet pair at physical distance $r = aR$, can be scaled between two points with scale ratio $\xi_{12} = a_2/a_1$ like

$$F_1(R) = \xi_{12}^{-2} F_2\left(\frac{R}{\xi_{12}}\right) \quad . \qquad \text{(III.8)}$$

If the static energy is determined for N different distances, the force represents (N-1) different physical quantities. Since the static energy can be obtained with good precision, Eq.(III.8) gives an accurate constraint on the RGT's. In fact, the scaling properties of the potential can be used in pure SU(2) gauge theory for the precise determination of the scale ratios ξ_{12} [27]. In the Higgs-model the shape of the potential changes gradually from Yukawa-type to a quasi-confinement form near the phase transition surface in the $(\lambda, \beta, \varkappa)$-space. Therefore, the RGT's can be pinned down by the requirement of a constant shape.

As it was discussed in detail in the previous and present Sections, the masses and static energies are universal functions of the link expectation value L independently from λ. This means that there exists a mapping between two planes $\lambda = \lambda_1$ and $\lambda = \lambda_2$ such, that the physical quantities do not change. Therefore, the coupling constant λ is irrelevant, there are only 2 relevant couplings. (Small deviations from universality may be due to lattice artifacts, and/or the optimal mapping can look a little bit different, for instance, there may be some small λ-dependent shift in β.) The numerical values of the masses and static energies obtained in Ref.[12] and here are all consistent with the assumption that the critical point in the $(\beta, \varkappa)$-plane (for fixed non-zero λ) is at $\beta = \infty, \varkappa = \varkappa_{cr}(\lambda)$. ($\varkappa_{cr}(\lambda)$ can be obtained in the σ-model at $\beta = \infty$.) For $0 \leq \varkappa < \varkappa_{cr}(\lambda)$ there are certainly the reduced critical points, equivalent to pure SU(2) gauge theory. Below the phase transition line in the $(\beta, \varkappa)$-plane, there might be also RGT's, which would correspond to a confining theory with scalar matter fields and zero vacuum expectation values (as advocated in Ref. [8]). In the present data we see no evidence for this, because everything measured below the phase transition line looks very similar to pure gauge theory. Nevertheless, in future Monte Carlo studies one should go very close to the phase transition line from below, perhapes also at larger β-values, in order to have better

constraints.

The present picture of RGT's is schematically represented by Fig. 15. As far as the general pattern is concerned, this is quite similar to the picture in QCD with a single dynamical quark mass. More information on the shape of the RGT's in the Higgs-phase can be obtained also from Fig. 12, where the curves of constant renormalized gauge coupling α are shown. Since the gauge coupling is asymptotically free, one expects that on a RGT α decreases for decreasing lattice spacing (i.e. for $\beta \to \infty$). Another way for the precise determination of the RGT's is a direct Monte Carlo renormalization group [28] study. In summary, one can say that in the two relevant couplings $(\beta, \varkappa)$, at arbitrarily fixed $\lambda > 0$, the renormalization group properties of the SU(2) fundamental Higgs-model look similar to the situation in QCD with a single dynamical quark mass.

The question naturally arises, what happens with the critical point at $\beta = \infty, \varkappa = \varkappa_{cr}(\lambda)$ for $\lambda \to 0$? This could again be a line of lower rank critical points (now with 2 relevant couplings) tending towards the next higher rank critical point at $\lambda = 0, \beta = \infty, \varkappa = 1/8$ (with 3 relevant couplings). Nevertheless, according to perturbation theory the λ coupling cannot be asymptotically free [29], therefore the existence of this critical point is rather doughtful.

IV. Conclusion

The numerical Monte Carlo study of correlations and static energies in the SU(2) gauge theory with a Higgs-scalar doublet turned out rather useful for the understanding of continuum physics behind the lattice-regularized theory. In this paper numerical evidence was found for the irrelevance of the Higgs self-coupling λ. The renormalization group properties in the two relevant couplings $(\beta, \varkappa)$ are qualitatively similar to the situation in QCD with a single (dynamical) quark mass. It is expected that for fixed λ there is a single critical point at $\beta = \infty, \varkappa = \varkappa_{cr}(\lambda)$ (where $\varkappa_{cr}(\lambda)$ is the critical point in the σ-model at $\beta = \infty$). In addition, for $\beta = \infty$, $0 \leq \varkappa < \varkappa_{cr}(\lambda)$

there is a line of reduced critical points, equivalent to pure SU(2) gauge theory.

In the ($\beta, \varkappa$)-plane, for any fixed $\lambda > 0$, the phase transition at the border of the Higgs-like phase is of first order. This is shown by a marked jump in both the W-boson and Higgs-boson mass. The renormalization group trajectories (RGT's) in the Higgs-phase tend to $\varkappa_{cr}(\lambda)$ from above for $\beta \to \infty$. Below the phase transition line, there might be RGT's describing a confining theory with scalar matter fields, but presently there is no evidence for this, since below the phase transition line every measured quantity looks very similar to pure SU(2) gauge theory.

The first order nature of the phase transition implies a lower bound for the ratio Higgs-mass to W-mass. The present numerical value of the bound is

$$\frac{m_H}{m_W} \geq 1.0 \pm 0.3 \quad . \tag{IV.1}$$

This relation holds also for weak gauge coupling (upto electromagnetic and fermionic corrections), because m_H / m_W increases with decreasing (renormalized) SU(2) gauge coupling.

The fact that there are only two relevant couplings implies, that the physical value of m_H / m_W is uniquely determined, if the renormalized gauge coupling is known. The direct Monte Carlo evaluation of m_H / m_W for the phenomenologically interesting weak coupling seems impossible. The best way is probably to go into the σ -model at $\beta = \infty$, and calculate m_W from the mass parameter f_g characterizing the spontaneous symmetry breaking SU(2) $\otimes$ SU(2) $\longrightarrow$ SU(2). (In the context of QCD f_g is usually denoted by f_π .) A possible way to extract f_g by Monte Carlo simulation in the σ -model was proposed recently by Dashen and Neuberger [16] . The numerical calculation seems not very easy, but it is certainly worth to try.

Acknowledgements. It is a pleasure to acknowledge the discussions with Peter Hasenfratz, Martin Lüscher and Roberto Peccei. Their remarks contributed in an essential way to the final form of this paper. I am indebted to Christian Lang for a correspondence about his Monte Carlo data. I wish to thank the Computer Centre of the University of Hamburg for the generous support of the computations in this paper.

References

[1] for a review and an extensive list of references see A. Peterman, Phys. Rep. 53C (1979) 157.

[2] J. C. Pati, A. Salam, Phys. Rev. Lett. 31 (1973) 661; Phys. Rev. D8 (1973) 1240;
H. Georgi, S. L. Glashow, Phys. Rev. Lett. 32 (1974) 438;
H. Georgi, H. Quinn, S. Weinberg, Phys. Rev Lett. 33 (1974) 451.

[3] UA1 Collaboration, Phys. Lett. 122B (1983) 103; 126B (1983) 398;
UA2 Collaboration, Phys. Lett. 122B (1983) 476; 129B (1983) 130.

[4] P. W. Higgs, Phys. Lett. 12 (1964) 132; Phys. Rev. Lett. 13 (1964) 508; Phys. Rev. 145 (1966) 1156;
F. Englert, R. Brout, Phys. Rev Lett. 13 (1964) 321;
G. S. Guralnik, C. R. Hagen, T. W. B. Kibble, Phys. Rev. Lett. 13 (1964) 585;
T. W. B. Kibble, Phys. Rev. 155 (1967) 1554.

[5] for references and a collection of papers see "Lattice gauge theories and Monte Carlo simulations" edited by C. Rebbi, World Scientific, 1983.

[6] P. V. D. Swift, Phys. Lett. 145B (1984) 256.

[7] K. G. Wilson, Phys. Rev. B4 (1971) 3184;
K. G. Wilson, J. Kogut, Phys. Rep. 12C (1974) 75;
R. Schrader, Phys. Rev. B14 (1976) 172;
B. Freedman, P. Smolensky, D. Weingarten, Phys. Lett. 113B (1982) 481;
M. Aizenmann, Phys. Rev. Lett. 47 (1981) 1; Commun. Math. Phys. 86 (1982) 1;
J. Fröhlich, Nucl. Phys. B200 [FS4] (1982) 281;
C. Aragao de Carvalho, C. S. Caracciolo, J. Fröhlich, Nucl. Phys. B215 [FS7] (1983) 209;
J. Fröhlich, in "Progress in gauge field theory" Cargèse lecture 1983, ed. G. 't Hooft et al., Plenum Press 1984.

[8] L. F. Abbott, E. Farhi, Phys. Lett. 101B (1981) 69.

[9] C. B. Lang, C. Rebbi, M. Virasoro, Phys. Lett. 104B (1981) 294;
M. Creutz, L. Jacobs, C. Rebbi, Phys. Rep. 95C (1983) 201.

[10] H. Kühnelt, C. B. Lang, G. Vones, Nucl. Phys. B230 [FS10] (1984) 31.

[11] M. Tomiya, T. Hattori, Phys. Lett. 140B (1984) 370.

[12] I. Montvay, Correlations in the SU(2) fundamental Higgs-model, to appear in Phys. Lett. B.

[13] E. Fradkin, S. Shenker, Phys. Rev. D19 (1979) 3682;
G. 't Hooft, Cargèse Summer Institute lecture, 1979;
T. Banks, E. Rabinivici, Nucl. Phys. B160 (1979) 349;
S. Dimopoulos, S. Raby, L. Susskind, Nucl. Phys. B173 (1980) 208.

[14] M. Veltman, Acta Phys. Polonica B8 (1977) 475;
B. W. Lee, C. Quigg, H. B. Thacker, Phys. Rev. D16 (1977) 1519;
T. Appelquist, C. Bernard, Phys. Rev. D22 (1980) 200;
A. Longhitano, Phys. Rev. D22 (1980) 1166.

[15] M. B. Einhorn, Nucl. Phys. B246 (1984) 75.

[16] R. Dashen, H. Neuberger, Phys. Rev. Lett. 50 (1983) 1897.

[17] M. Gell-Mann, M. Lévy, Nuovo Cimento, 16 (1960) 705.

[18] W. A. Bardeen, M. Moshe, Phys. Rev. D28 (1983) 1372.

[19] see for instance B. Berg, S. Meyer, I. Montvay, Nucl. Phys. B235 [FS11] (1984) 149 and references therein.

[20] see for instance H. Meyer-Ortmanns, I. Montvay, Phys. Lett. 145B (1984) 251 and references therein.

[21] Aachen-group lecture presented by T. Neuhaus at the CERN Lattice Meeting (December 1984).

[22] S. Coleman, E. Weinberg, Phys. Rev. D7 (1973) 1888.

[23] M. Peskin, Annals of Phys. (N. Y.) 113 (1978) 122.

[24] I. Montvay, lecture given at the 1984 Aspen Center for Physics, to be published in Rev. Mod. Phys.

[25] E. L. Berger, M. Jacob, Phys. Lett. 147B (1984) 197.

[26] B. Schrempp, F. Schrempp, DESY preprint 84-117(1984) and references therein.

[27] F. Gutbrod, I. Montvay, Phys. Lett. 136B (1984) 411.

[28] S. K. Ma, Phys. Rev. Lett. 37 (1976) 461;
R. H. Swendsen, Phys. Rev. Lett. 42 (1979) 859;
K. G. Wilson, in"Recent developments of gauge theories, ed. G. 't Hooft et al., Plenum Press, 1980;
A. Hasenfratz, P. Hasenfratz, U. Heller, F. Karsch, Phys. Lett. 140B (1984) 76.

[29] D. J. E. Callaway, Nucl. Phys. B233 (1984) 189.

[30] W. Langguth, I. Montvay, Phys. Lett. 145B (1984) 261.

Table I.

The values of the W-boson mass (am_W) and Higgs-boson mass (am_H) in lattice units. The global average quantities L, P, ρ, σ_ρ and χ are defined in Eq.(II.18). The errors in the last numerals are given in paranthesis. If no error is given, the error estimate is ≤ 1 in the last digit. The β -value is always $\beta = 2.3$. The lines with an asterisk were obtained with full SU(2) group, the rest with the icosahedral subgroup.

λ	κ	am_W	am_H	L	P	χ	ρ	σ_ρ
∞	0.35	2.5(5)	1.51(15)	0.2011(3)	0.3954(4)	8.693(5)		
∞	0.38	2.4(4)	1.27(9)	0.2318(4)	0.3931(6)	8.760(6)		
∞	0.4	0.79(8)	0.59(12)	0.2948(26)	0.3820(13)	8.528(15)		
∞	0.42	0.65(7)	1.08(12)	0.3437(11)	0.3757(3)	8.390(4)		
∞	0.45	0.62(11)	1.4(2)	0.3993(3)	0.3696(5)	8.263(6)		
∞	0.5*	0.60(7)	1.5(2)	0.4669(4)	0.3623(3)	8.132(4)		
∞	0.6*	0.67(11)	1.7(3)	0.5574(2)	0.3512(3)	7.971(3)		
∞	0.8*	0.89(9)	2.1(3)	0.6596(2)	0.3348(3)	7.799(4)		
1.0	0.2	4.0(5)	1.12(16)	0.1181(3)	0.3973(2)	8.300(6)	1.060	0.260
1.0	0.3	1.8(3)	1.09(8)	0.2316(2)	0.3924(2)	8.547(3)	1.115	0.258
1.0	0.31	0.73(12)	0.98(10)	0.3216(4)	0.3772(3)	8.080(7)	1.152	0.250(2)
1.0	0.32	0.56(6)	1.16(12)	0.3786(6)	0.3709(2)	7.821(9)	1.178	0.252(2)
1.0	0.35	0.67(7)	1.55(16)	0.4919(4)	0.3583(2)	7.256(6)	1.241	0.243
1.0	0.4	0.83(7)	1.72(18)	0.6101(5)	0.3425(2)	6.432(9)	1.331	0.228
0.5	0.25	2.7(5)	1.25(14)	0.1957(6)	0.3951(3)	8.318(6)	1.164	0.306
0.5	0.3	0.68(7)	1.34(18)	0.5009(3)	0.3569(2)	6.821(8)	1.358	0.292
0.1	0.19	2.5(5)	1.26(11)	0.2064(2)	0.3939(2)	7.775(11)	1.353	0.420
0.1	0.195	0.45(9)	0.50(12)	0.3159(3)	0.3771(2)	7.220(32)	1.450	0.429
0.1	0.2	0.53(7)	0.98(12)	0.4238(8)	0.3650(4)	6.673(15)	1.558	0.433
0.1	0.205	0.53(6)	1.21(14)	0.4879(5)	0.3577(2)	6.301(9)	1.636	0.432
0.1	0.21	0.72(7)	1.46(19)	0.5428(3)	0.3510	5.939(3)	1.712	0.427
0.1	0.22	0.85(7)	1.48(19)	0.6199(6)	0.3399(2)	5.298(10)	1.845	0.410
0.1	0.3	1.47(7)	2.4(3)	0.8415(2)	0.2728	0.187	2.628	0.327

Table II.

The values of am_q and am_h for $\beta = \infty$. The average quantities L, ρ, σ_ρ and χ are defined in Eq.(II.20). The errors in the last numerals are given in paranthesis. If no error is given, the error estimate is ≤ 1 in the last digit.

λ	κ	am_q	am_h	L	χ	ρ	σ_ρ
1.0	0.22	0.78(6)	1.91(11)	0.1436(6)	2.570	1.070	0.258
1.0	0.24	0.33(4)	1.14(9)	0.1717(3)	2.526	1.081	0.259
1.0	0.25	0.04(2)	0.44(7)	0.2198(12)	2.297(6)	1.092	0.255
1.0	0.26	0.03(2)	0.71(9)	0.2954(14)	1.890(2)	1.124	0.256
1.0	0.27	0.02(2)	0.99(8)	0.3620(6)	1.467(8)	1.1490(4)	0.256
1.0	0.28	0.04(2)	1.31(14)	0.4180(9)	1.072(4)	1.173	0.249
1.0	0.3	0.03(2)	1.52(15)	0.5070(6)	0.297(5)	1.216	0.245
1.0	0.32	0.02(2)	1.85(16)	0.6361(4)	-0.485(3)	1.256	0.241
0.1	0.155	0.51(5)	1.42(14)	0.1512(3)	1.918(2)	1.2901(8)	0.410
0.1	0.16	0.22(4)	0.92(11)	0.1664(4)	1.845(8)	1.3022(6)	0.413
0.1	0.163	0.08(3)	0.46(7)	0.1896(2)	1.735(3)	1.3191(2)	0.415
0.1	0.165	0.04(2)	0.37(8)	0.2269(5)	1.522(6)	1.346	0.417
0.1	0.167	0.02(2)	0.48(6)	0.2733(15)	1.256(9)	1.3793(7)	0.421
0.1	0.17	0.04(3)	0.81(8)	0.3401(12)	0.800(5)	1.430	0.426
0.1	0.175	0.03(2)	0.94(12)	0.4344(5)	0.065(3)	1.514	0.427
0.1	0.18	0.02(2)	1.21(11)	0.5079(14)	-0.640(2)	1.5891(6)	0.427

Table IIIA.

The expectation value of Wilson-loops W_{RT} in units of 10^{-5}.

λ	β	$\varkappa$	W_{11}	W_{12}	W_{13}	W_{14}	W_{15}
∞	2.0	0.55	57142(12)	35651(20)	22770(20)	14640(18)	9435(17)
∞	2.1	0.5	58983(9)	37855(14)	24833(15)	16384(14)	10827(12)
∞	2.1	0.6	60832(7)	40634(10)	27774(11)	19094(10)	13145(10)
∞	2.1	0.8	63142(7)	44145(10)	31524(11)	22647(11)	16287(11)
∞	2.3	0.3	60349(12)	38768(18)	25247(21)	16496(18)	10789(16)
∞	2.3	0.4	61805(10)	41123(16)	27848(19)	18946(18)	12906(17)
∞	2.3	0.45	63022(9)	43099(13)	30055(15)	21066(15)	14787(14)
∞	2.3	0.5	63759(6)	44257(9)	31339(10)	22306(10)	15900(10)
∞	2.3	0.6	64885(6)	46021(10)	33314(11)	24233(12)	17644(12)
∞	2.3	0.8	66529(6)	48599(8)	36215(9)	27106(10)	20316(10)
∞	2.4	0.4	64259(8)	44586(13)	31500(14)	22354(14)	15883(13)
∞	2.4	0.5	65631(6)	46819(10)	34052(11)	24883(11)	18206(11)
∞	2.4	0.6	66547(5)	48282(8)	35711(11)	26536(12)	19742(13)
∞	2.5	0.4	66155(8)	47246(12)	34341(14)	25073(16)	18328(16)
∞	2.5	0.45	66784(10)	48275(14)	35530(17)	26267(18)	19442(18)
1.0	2.3	0.32	62896(9)	42880(15)	29806(17)	20829(17)	14582(16)
1.0	2.3	0.35	64153(10)	44866(16)	32021(21)	22970(23)	16502(21)
1.0	2.3	0.4	65753(6)	47378(8)	34835(9)	25736(9)	19038(9)
0.1	2.3	0.195	62428(11)	42129(18)	28970(20)	20021(19)	13861(17)
0.1	2.3	0.205	64233(9)	44999(14)	32166(16)	23116(15)	16634(13)
0.1	2.3	0.22	66004(8)	47772(12)	35280(14)	26179(15)	19447(15)

Table IIIB.

The expectation value of Wilson-loops W_{RT} in units of 10^{-5}.

λ	β	$\varkappa$	W_{22}	W_{23}	W_{24}	W_{25}	W_{55}
∞	2.0	0.55	16925(22)	8881(20)	4833(18)	2661(8)	274(8)
∞	2.1	0.5	18783(18)	10212(15)	5722(12)	3238(10)	385(7)
∞	2.1	0.6	22101(13)	13111(12)	7982(11)	4890(9)	850(7)
∞	2.1	0.8	26323(12)	16984(12)	11168(11)	7382(10)	1794(8)
∞	2.3	0.3	18187(23)	9030(22)	4555(15)	2303(11)	71(5)
∞	2.3	0.4	21263(23)	11814(23)	6715(18)	3858(15)	351(7)
∞	2.3	0.45	23873(18)	14268(16)	8731(14)	5386(12)	835(8)
∞	2.3	0.5	25380(13)	15696(13)	9928(11)	6324(11)	1189(10)
∞	2.3	0.6	27666(13)	17895(12)	11806(12)	7828(11)	1799(9)
∞	2.3	0.8	31013(11)	21161(11)	14677(10)	10225(9)	2958(9)
∞	2.4	0.4	25113(19)	15163(19)	9352(16)	5812(13)	859(10)
∞	2.4	0.5	28145(13)	18149(14)	11934(13)	7901(12)	1722(9)
∞	2.4	0.6	30101(12)	20072(13)	13627(12)	9300(11)	2379(10)
∞	2.5	0.4	28083(17)	17822(18)	11532(18)	7522(16)	1388(11)
∞	2.5	0.45	29512(20)	19260(20)	12810(18)	8570(16)	1885(11)
1.0	2.3	0.32	23575(21)	13988(20)	8500(17)	5208(14)	785(10)
1.0	2.3	0.35	26154(20)	16441(21)	10552(19)	6820(15)	1373(13)
1.0	2.3	0.4	29430(9)	19603(9)	13295(9)	9063(8)	2371(8)
0.1	2.3	0.195	22586(23)	13041(23)	7712(17)	4595(13)	575(10)
0.1	2.3	0.205	26327(19)	16604(20)	10698(16)	6939(14)	1420(10)
0.1	2.3	0.22	29939(16)	20100(16)	13737(14)	9431(12)	2565(11)

Table IIIC.

The expectation value of Wilson-loops W_{RT} in units of 10^{-5}.

λ	β	$\varkappa$	W_{33}	W_{34}	W_{35}	W_{44}	W_{45}
∞	2.0	0.55	4247(21)	2171(13)	1130(7)	1101(8)	553(7)
∞	2.1	0.5	5059(14)	2658(9)	1430(7)	1356(9)	720(6)
∞	2.1	0.6	7316(13)	4284(10)	2554(7)	2470(9)	1447(6)
∞	2.1	0.8	10561(12)	6790(10)	4401(8)	4333(10)	2795(8)
∞	2.3	0.3	3617(18)	1510(12)	626(8)	511(6)	179(5)
∞	2.3	0.4	5798(18)	2999(14)	1579(10)	1459(11)	731(8)
∞	2.3	0.45	7869(16)	4558(12)	2684(9)	2562(11)	1479(8)
∞	2.3	0.5	9092(13)	5503(10)	3379(9)	3255(10)	1981(8)
∞	2.3	0.6	11023(13)	7051(11)	4552(8)	4453(11)	2851(8)
∞	2.3	0.8	13960(12)	9478(11)	6479(9)	6376(10)	4342(8)
∞	2.4	0.4	8374(18)	4833(14)	2835(12)	2681(11)	1531(9)
∞	2.4	0.5	11045(14)	6989(12)	4472(9)	4339(10)	2739(8)
∞	2.4	0.6	12784(13)	8423(11)	5607(10)	5471(11)	3617(10)
∞	2.5	0.4	10492(18)	6434(16)	4008(12)	3822(14)	2331(10)
∞	2.5	0.45	11832(20)	7549(16)	4875(15)	4721(17)	3002(13)
1.0	2.3	0.32	7615(18)	4352(14)	2539(11)	2415(13)	1386(9)
1.0	2.3	0.35	9749(19)	6022(16)	3767(13)	3651(19)	2248(14)
1.0	2.3	0.4	12541(11)	8286(10)	5529(8)	5425(10)	3580(9)
0.1	2.3	0.195	6814(22)	3752(16)	2113(11)	1981(15)	1079(10)
0.1	2.3	0.205	9870(18)	6116(15)	3844(11)	3721(15)	2306(11)
0.1	2.3	0.22	12991(15)	8670(14)	5830(12)	5726(14)	3839(11)

Table IV.

Parameters of the potential in a Yukawa-(Y), Hulthén-(H) and string-like(S) fit defined by Eq.(III.3). The errors in paranthesis are the sums of satistical errors and estimated systematic errors.

λ	β	$\varkappa$	fit	α	c	am	$a^2\sigma$
∞	2.0	0.55	S	0.305(15)	0.75(2)		0.003(3)
∞	2.1	0.5	Y,H	0.312(14)	0.66(2)	0.41(12)	
∞	2.1	0.6	Y,H	0.258(9)	0.538(4)	0.64(18)	
∞	2.1	0.8	Y,H	0.214(9)	0.441(2)	0.91(21)	
∞	2.3	0.3	S	0.192(22)	0.46(3)		0.160(10)
∞	2.3	0.4	S	0.274(8)	0.63(1)		0.032(3)
∞	2.3	0.45	S	0.250(5)	0.60(1)		0.002(2)
∞	2.3	0.5	Y,H	0.234(6)	0.52(1)	0.42(16)	
∞	2.3	0.6	Y,H	0.207(6)	0.453(2)	0.61(18)	
∞	2.3	0.8	Y,H	0.178(5)	0.387(1)	0.82(22)	
∞	2.4	0.4	S	0.241(5)	0.571(6)		0.0118(17)
∞	2.4	0.5	Y,H	0.206(5)	0.477(6)	0.33(15)	
∞	2.4	0.6	Y,H	0.191(5)	0.421(2)	0.60(19)	
∞	2.5	0.4	S	0.213(4)	0.519(5)		0.0067(14)
∞	2.5	0.45	Y,H	0.201(3)	0.48(1)	0.18(9)	
1.0	2.3	0.32	Y,H	0.264(3)	0.61(1)	0.14(7)	
1.0	2.3	0.35	Y,H	0.218(7)	0.50(1)	0.38(15)	
1.0	2.3	0.4	Y,H	0.187(5)	0.417(2)	0.69(21)	
0.1	2.3	0.195	S	0.277(5)	0.64(1)		0.0089(21)
0.1	2.3	0.205	Y,H	0.218(6)	0.49(1)	0.44(19)	
0.1	2.3	0.22	Y,H	0.190(6)	0.404(1)	0.81(25)	

Figure captions

Fig. 1. The phase transition lines in the $(g^{-2}, \varkappa)$-plane for constant λ according to Fig. 3 in Ref. [10].

Fig. 2A. The inverse correlation lengths in the W-boson (am_W) and Higgs-boson (am_H) channel in lattice units for $\lambda = \infty$, $\beta = 2.3$.

Fig. 2B. The same as Fig. 2A, for $\lambda = 1.0$, $\beta = 2.3$.

Fig. 2C. The same as Fig. 2A, for $\lambda = 0.1$, $\beta = 2.3$.

Fig. 3. The link expectation value $L = \langle \frac{1}{2} \mathrm{Tr} V_l \rangle$ as a function of the plaquette expectation value $P = \langle 1 - \frac{1}{2} \mathrm{Tr} V_\square \rangle$ for different λ -values at $\beta = 2.3$.

Fig. 4A. The W-boson mass in lattice units (am_W) as a function of the link expectation value $L = \langle \frac{1}{2} \mathrm{Tr} V_l \rangle$ for different λ -values at $\beta = 2.3$.

Fig. 4B. The same as Fig. 4A, for the Higgs-boson mass (am_H).

Fig. 5. The $\varkappa$ -dependence of the average link $L = \langle \frac{1}{2} \mathrm{Tr} V_l \rangle$, average plaquette $P = \langle 1 - \frac{1}{2} \mathrm{Tr} V_\square \rangle$ and average action per point $S = \langle S \rangle$ as defined in Eq.(II.18), for $\lambda = \infty$, $\beta = 2.3$. The lines are drawn just to guide the eye.

Fig. 6A. The inverse correlation lengths in the Goldstone-boson (am_g) and Higgs-boson (am_h) channel in lattice units in the σ -model at $\beta = \infty$ for $\lambda = 1.0$.

Fig. 6B. The same as Fig. 6A, for $\lambda = 0.1$.

Fig. 7. The inverse correlation lengths in the σ -model at $\beta = \infty$ plotted as a function of the average link $L = \langle \frac{1}{2} \mathrm{Tr} V_l \rangle$ defined in Eq.(II.2o).

Fig. 8. Typical examples of the static potential aE in such points, where the Yukawa-form gives a good fit.

Fig. 9. The gradual change of the potential shape near the phase transition surface on the border of the Higgs-like region. The transition for $\lambda = \infty, \beta = 2.3$ is at $\varkappa_{cr} = 0.386 \pm 0.005$.

Fig. 10A. An example of the potential, where the Yukawa-fit (dashed line) is much worse than the string-potential fit (full line). Note, that the best Yukawa-fit gives a mass $am \leq 0.0$, whereas the W-boson mass measured from the correlations is $am_W = 0.45 \pm 0.09$.

Fig. 10B. Another example, where the Yukawa-fit (dashed line) to the potential is very bad, but the string-potential fit (full line) is quite good. Note also here, that the best Yukawa-fit requires $am = 0$, whereas the W-boson mass obtained from the correlations is $am_W = 0.79 \pm 0.08$.

Fig. 11. The static potential in a point ($\lambda = \infty$, $\beta = 2.3$, $\varkappa = 0.3$) below the phase transition surface ($\varkappa < \varkappa_{cr}$).

Fig. 12. The curves of constant renormalized gauge coupling (α) for $\lambda = \infty$ in the ($\beta, \varkappa$)-plane. The lines were obtained from the potential fits given in Table IV by a linear interpolation. The point P gives the position of the phase transition at $\lambda = \infty$, $\beta = 2.3$.

Fig. 13. Comparison of the static potential extracted from the expectation values of Wilson-loops and "chiral" loops. All the points shown were obtained from the ratio of loops with time-elongation T=3 and 5.

Fig. 14. The expected shape of the scaling region in the (β, μ_q)-plane for QCD with $N_f = 3$ degenerate quark flavours. β is the SU(3) gauge coupling and μ_q is the quark mass parameter for Wilson-fermions. The shape of the RGT's for small and large RG invariant quark mass M_q is shown. The meaning of the other curves is explained in the text. A spectrum calculation with dynamical quarks was performed in Ref. [30] for ($\beta = 5.4$; $\mu_q = 3.0675$) and ($\beta = 5.3$; $\mu_q = 2.9762$). These points are denoted, respectively, by A and B. The RGT's with constant M_q and the critical line $\mu_{cr}(\beta)$ tend for $\beta \to \infty$ to $\mu_q = 4$.

Fig. 15. The schematic behaviour of the renormalization group trajectories in the ($\beta_1 \varkappa$)-plane for any λ =const.>0 . The phase transition line is dashed-dotted. The full lines are the RGT's in the Higgs-like phase. The dashed lines could be RGT's in the confinement-like phase, which tend to the critical point below the phase transition line.

Fig.1

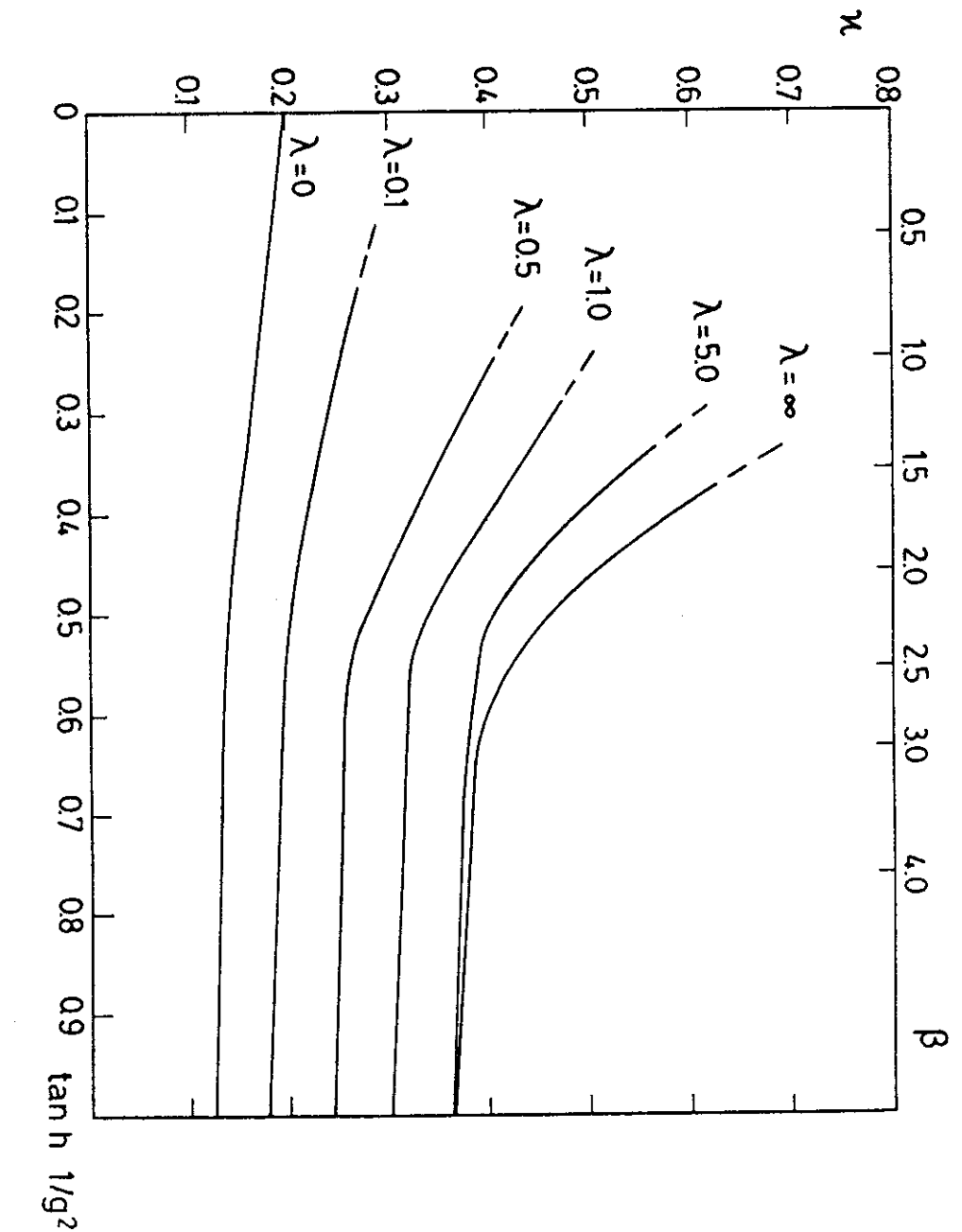

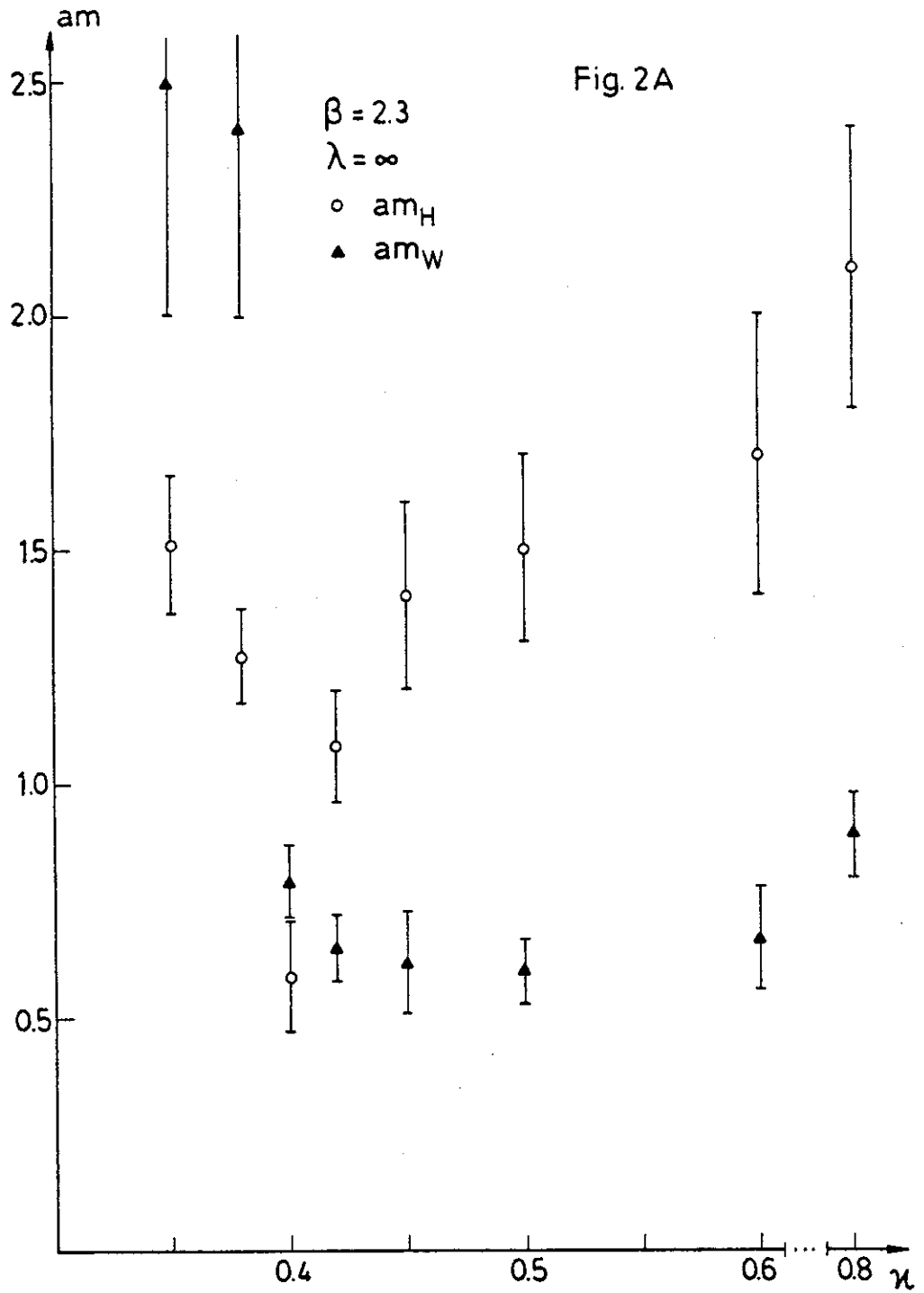
am
2.5
2.0
1.5
1.0
0.5
β = 2.3
λ = ∞
am_H
am_W
0.4
0.5
0.6
0.8
κ

Fig. 2A

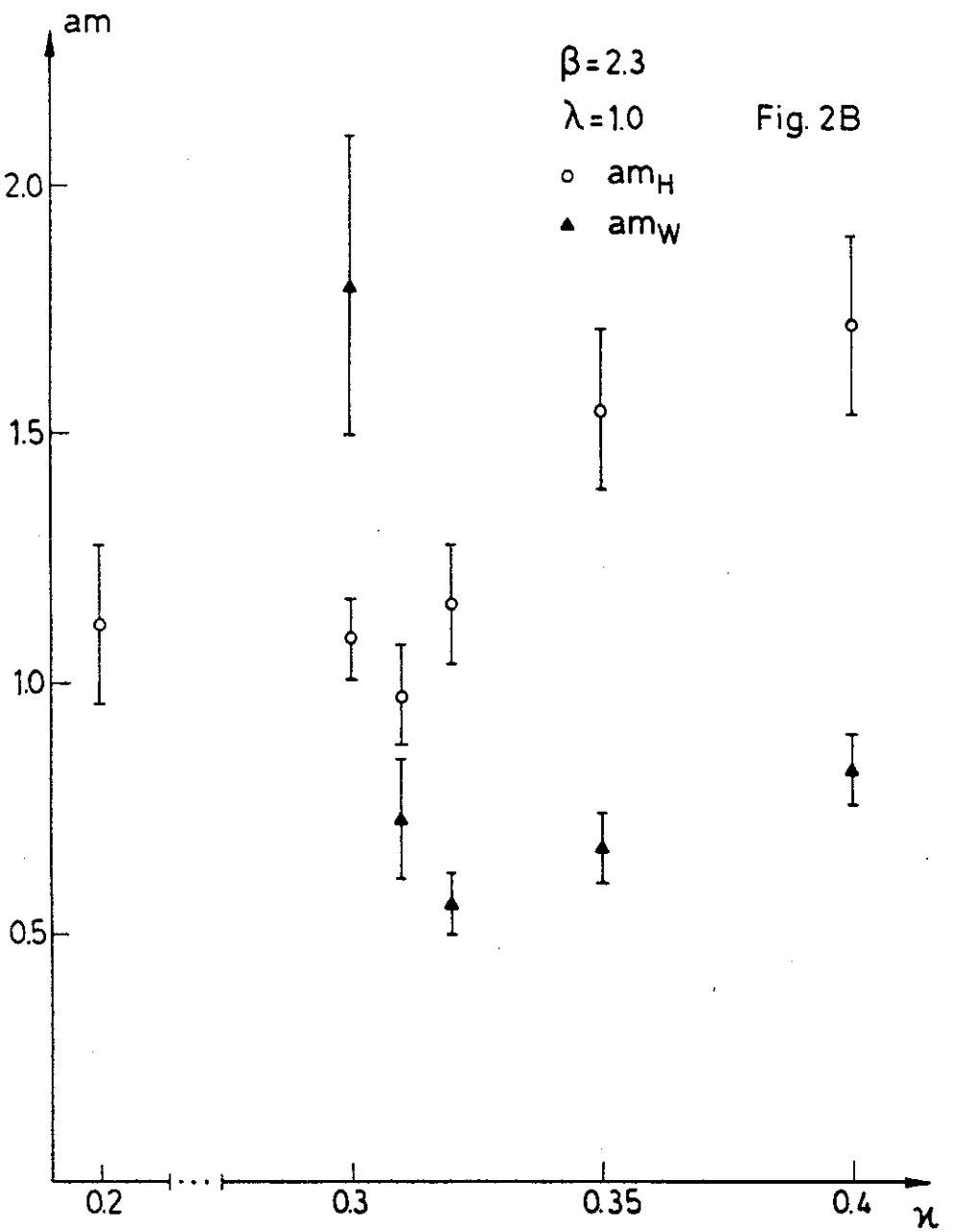
am
2.0
1.5
1.0
0.5
β = 2.3
λ = 1.0
am_H
am_W
0.2
0.3
0.35
0.4
κ

Fig. 2B

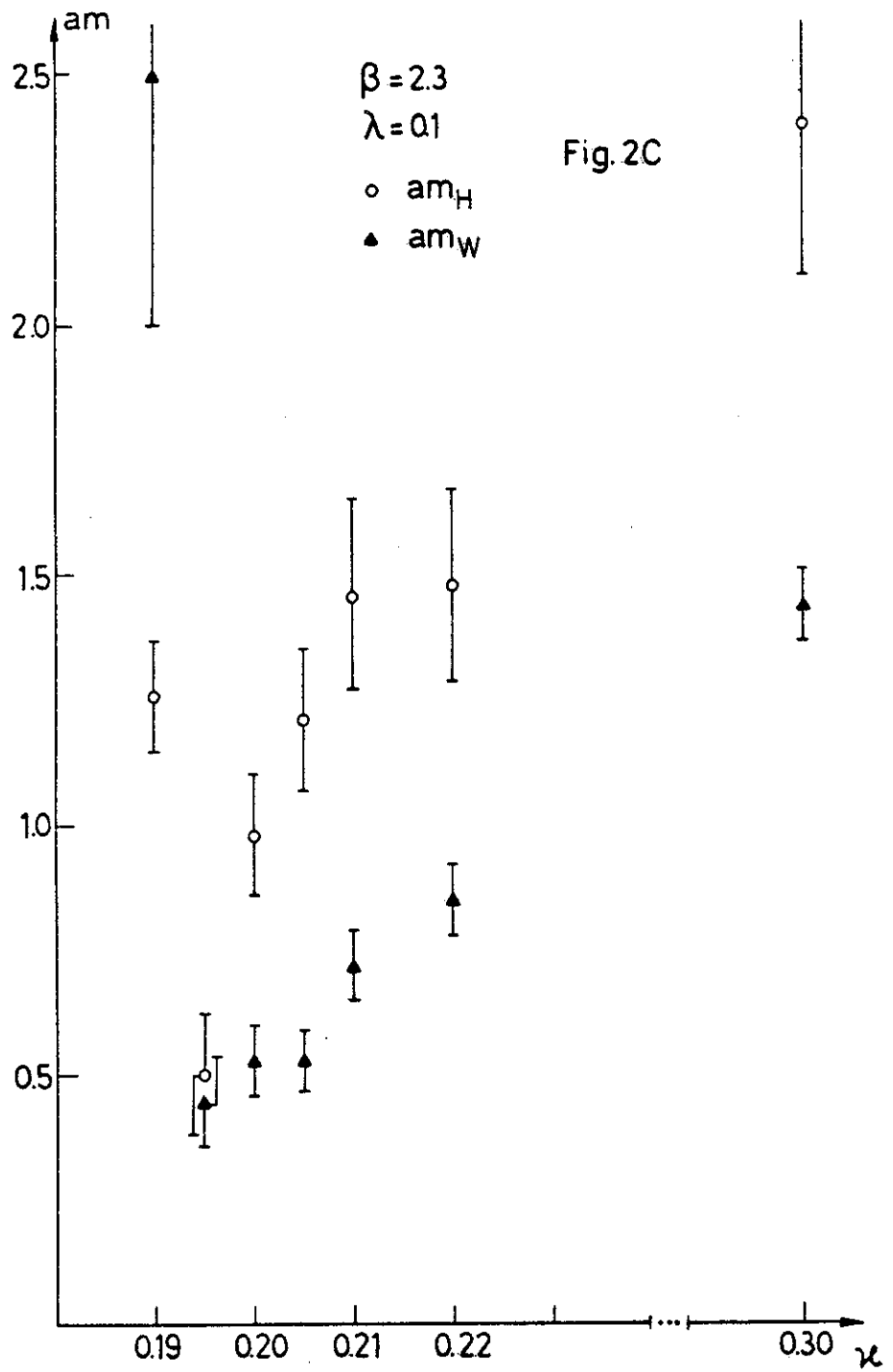
am
2.5
2.0
1.5
1.0
0.5
β = 2.3
λ = 0.1
am_H
am_W
0.19
0.20
0.21
0.22
0.30
κ

Fig. 2C

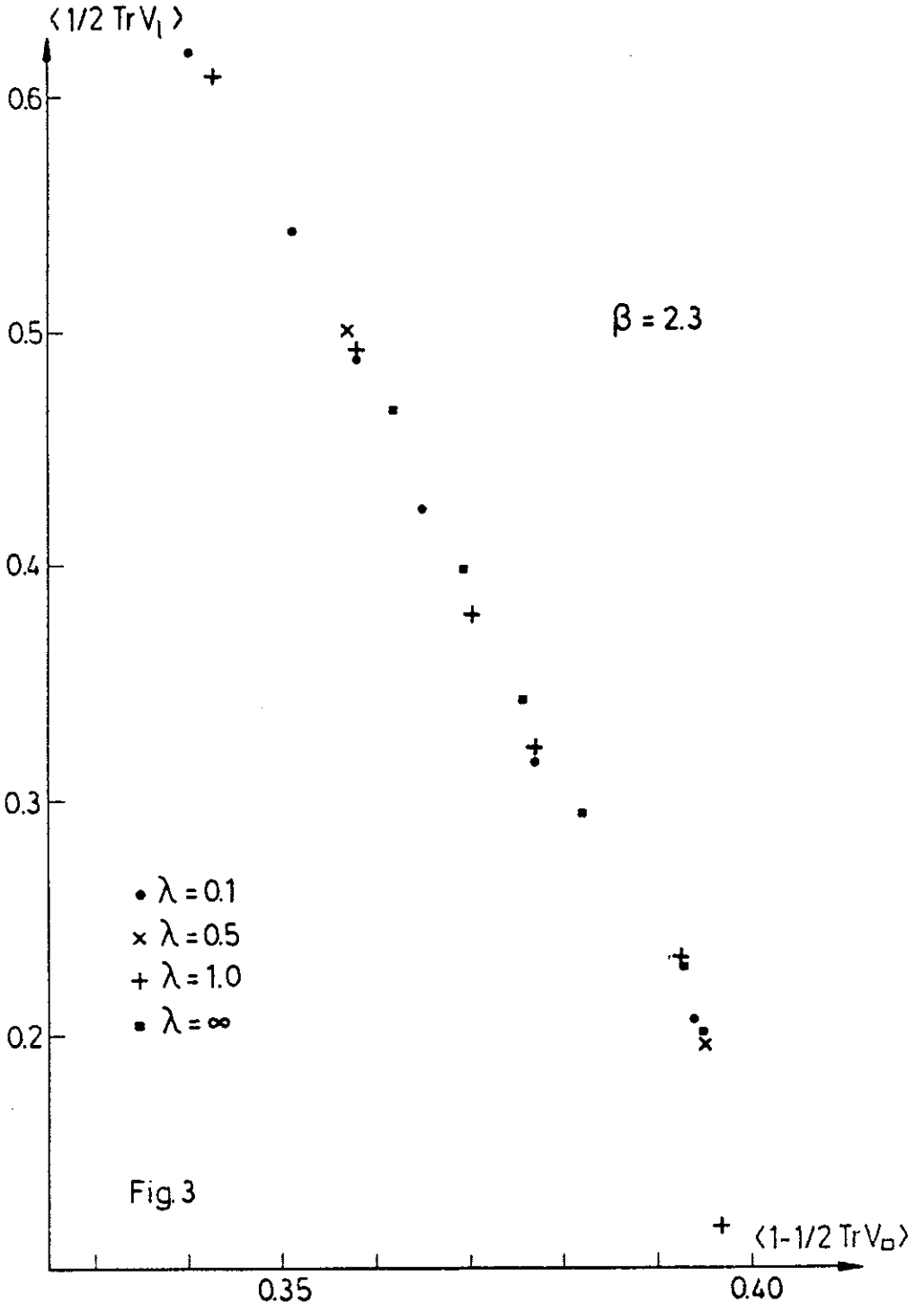
⟨1/2 Tr V_l⟩
0.6
0.5
0.4
0.3
0.2
β = 2.3
• λ = 0.1
× λ = 0.5
+ λ = 1.0
▪ λ = ∞
0.35
0.40
⟨1-1/2 Tr V_□⟩

Fig. 3

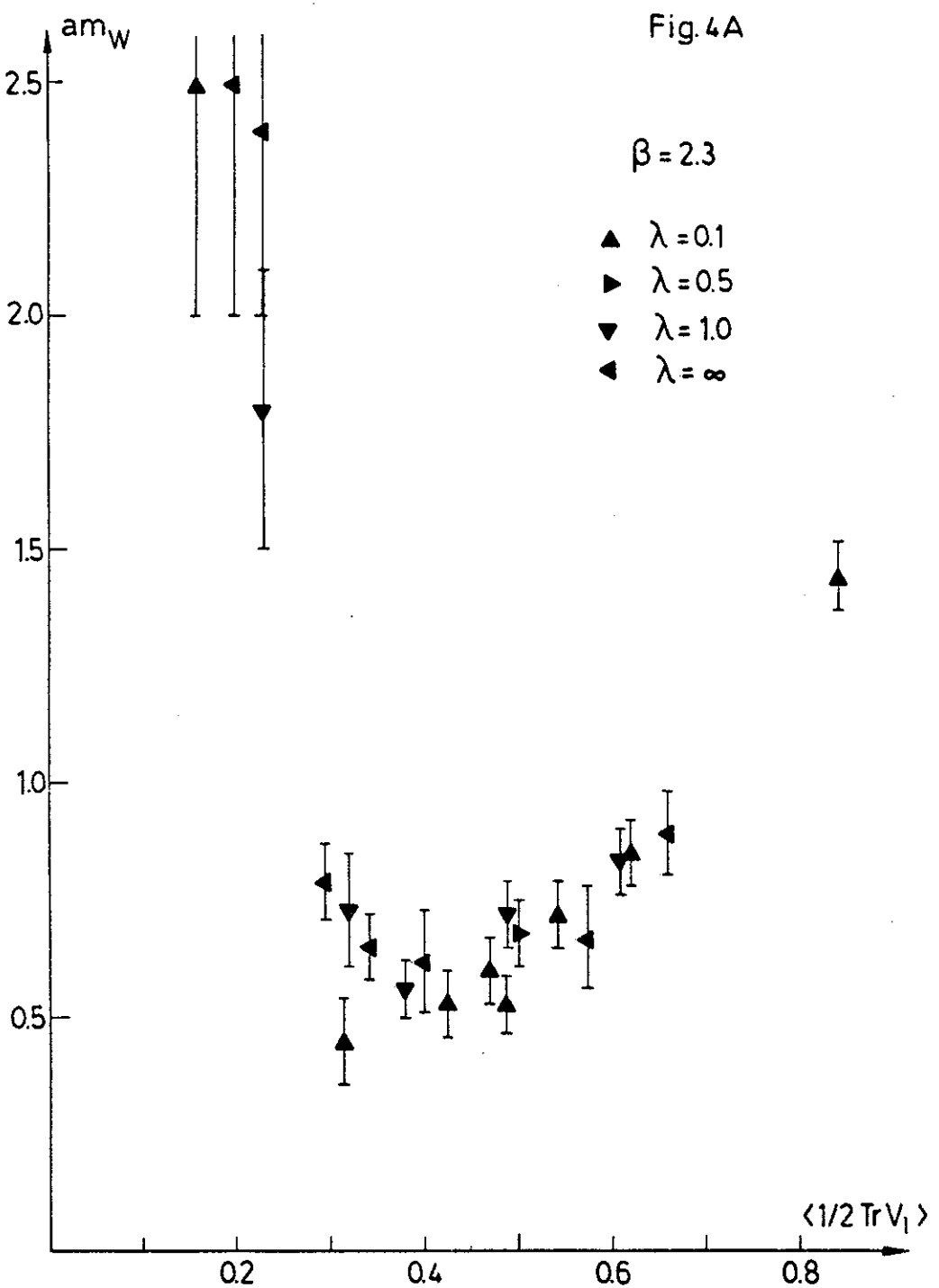
Fig. 4A
am_W
2.5
2.0
1.5
1.0
0.5
$\beta = 2.3$
$\lambda = 0.1$
$\lambda = 0.5$
$\lambda = 1.0$
$\lambda = \infty$
$\langle 1/2\ Tr\ V_l \rangle$
0.2
0.4
0.6
0.8

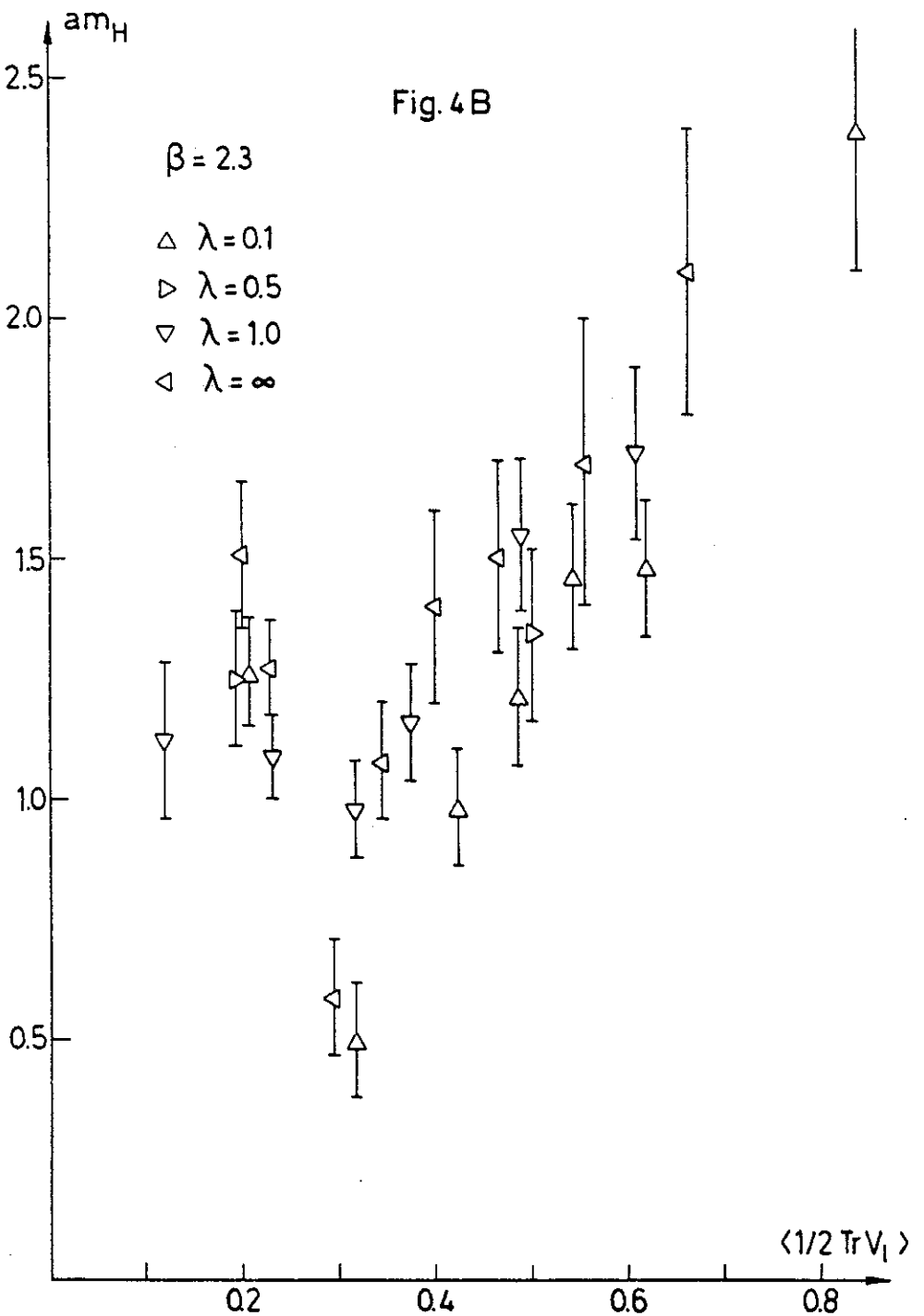
Fig. 4B
am_H
2.5
2.0
1.5
1.0
0.5
$\beta = 2.3$
$\lambda = 0.1$
$\lambda = 0.5$
$\lambda = 1.0$
$\lambda = \infty$
$\langle 1/2\ Tr\ V_l \rangle$
0.2
0.4
0.6
0.8

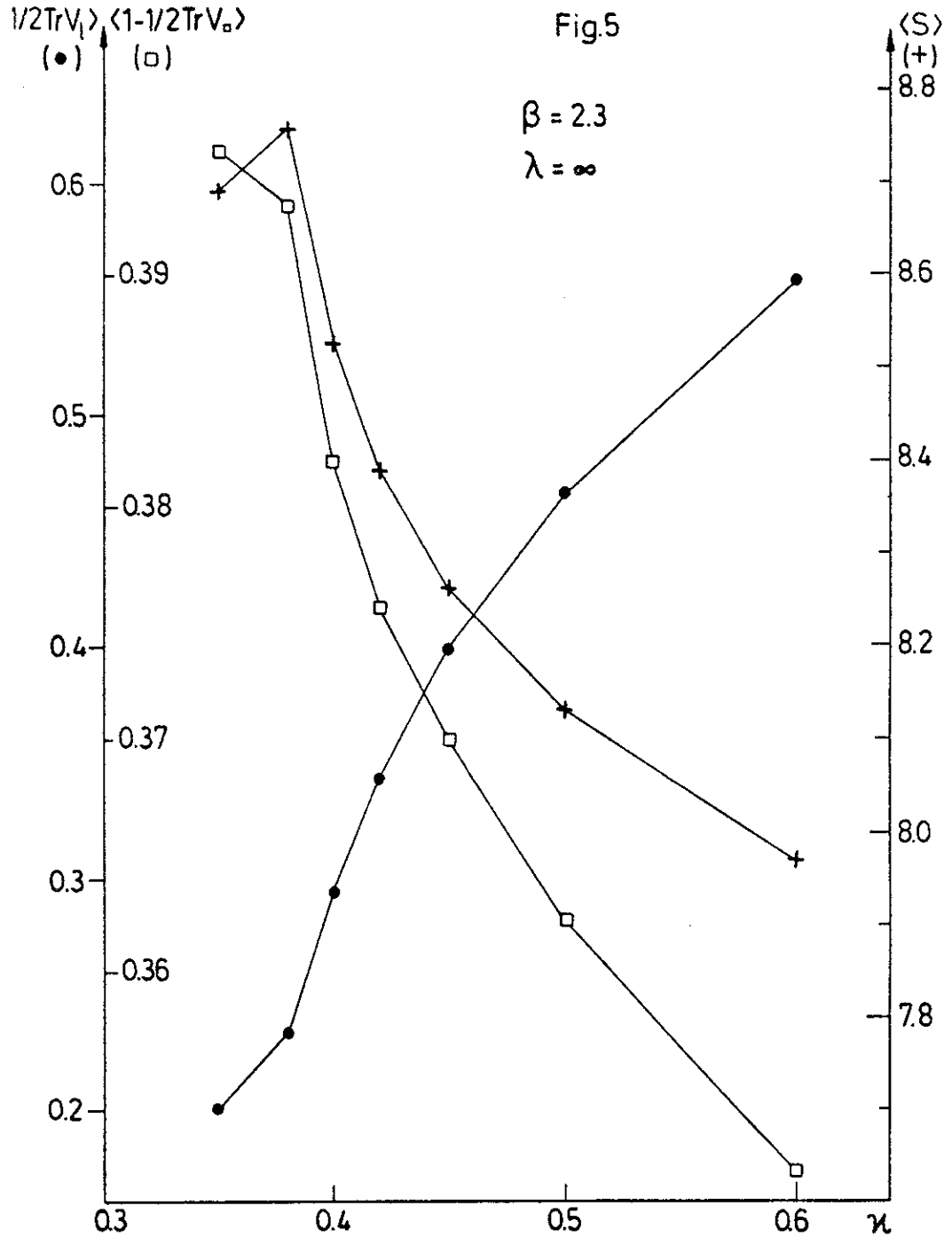
1/2TrV_t⟩ ⟨1-1/2TrV_s⟩
(●) (□)
⟨S⟩
(+)
β = 2.3
λ = ∞
0.6
0.5
0.4
0.3
0.2
0.39
0.38
0.37
0.36
8.8
8.6
8.4
8.2
8.0
7.8
0.3
0.4
0.5
0.6
κ

Fig.5

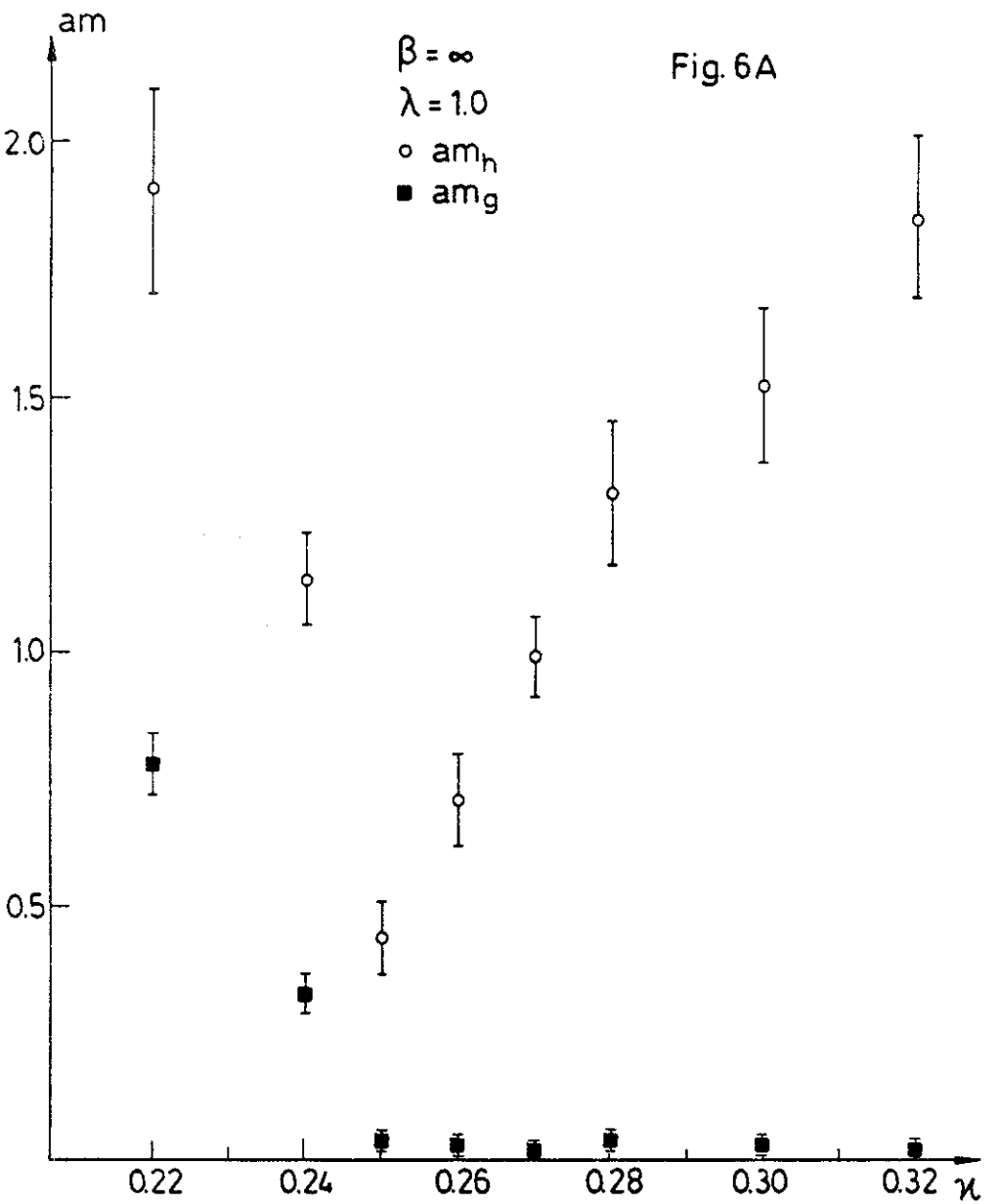
am
β = ∞
λ = 1.0
○ am_h
■ am_g
2.0
1.5
1.0
0.5
0.22
0.24
0.26
0.28
0.30
0.32
κ

Fig. 6A

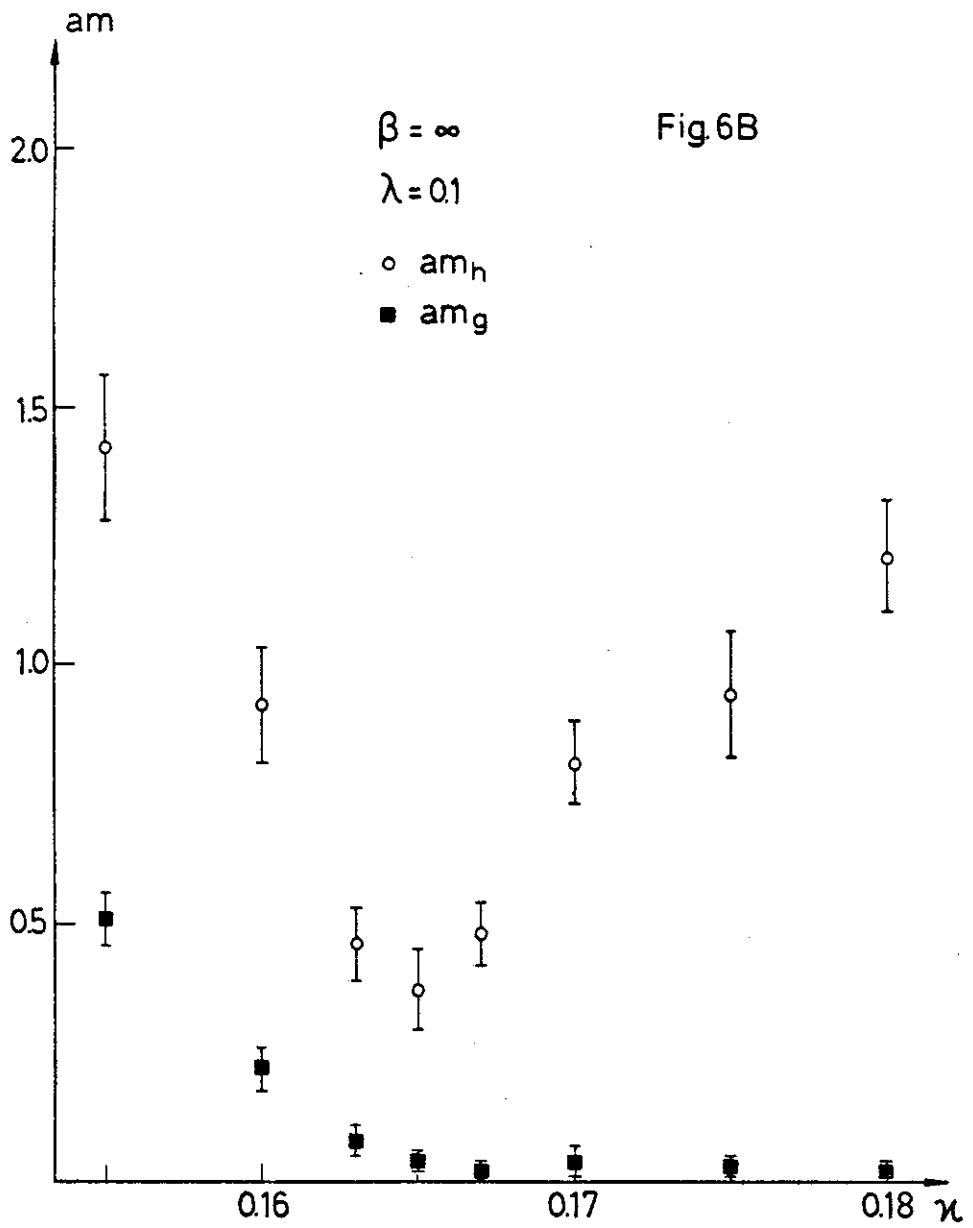
am
2.0
1.5
1.0
0.5
β = ∞
λ = 0.1
am_h
am_g
0.16
0.17
0.18
κ

Fig. 6B

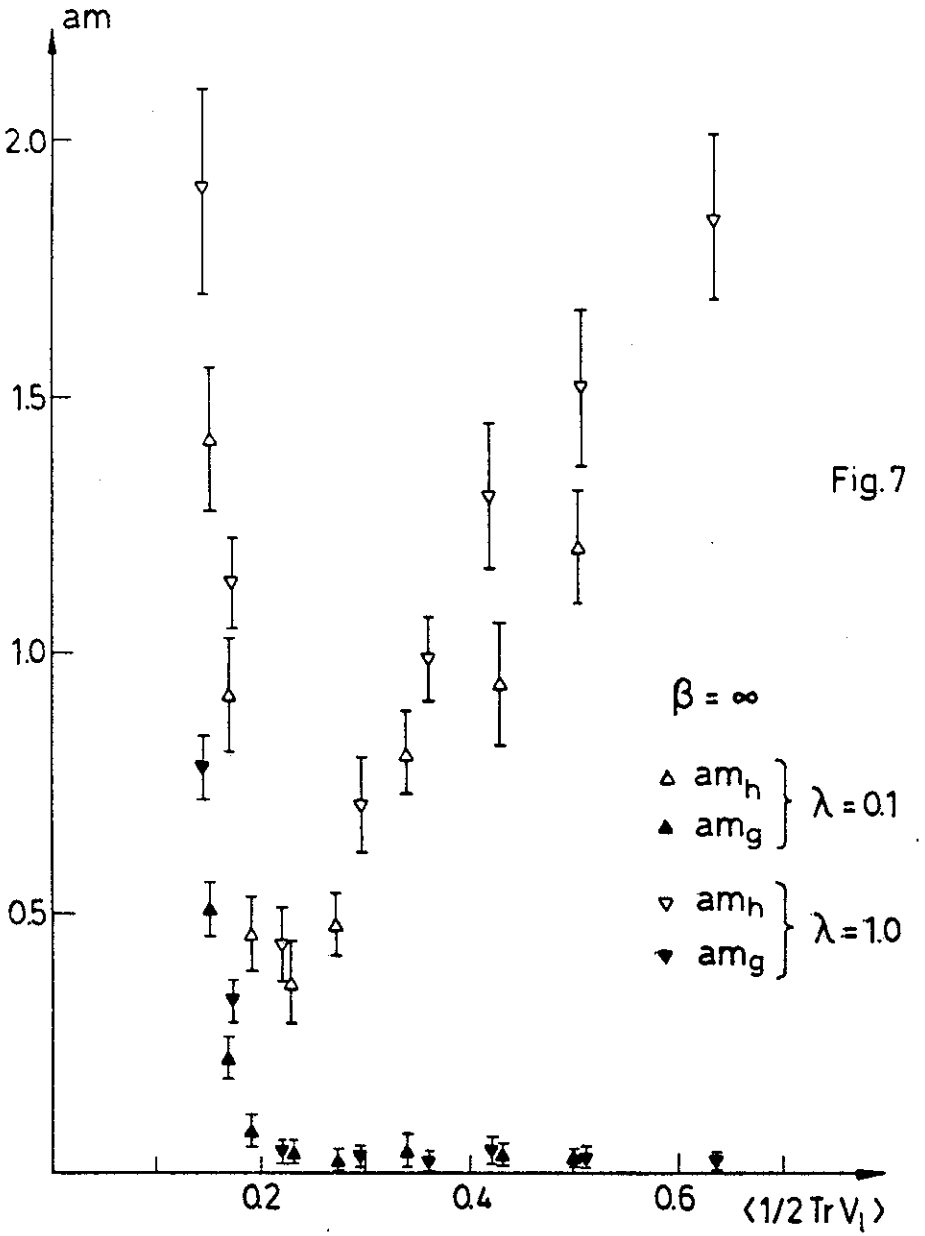
am
2.0
1.5
1.0
0.5
β = ∞
am_h
am_g
λ = 0.1
am_h
am_g
λ = 1.0
0.2
0.4
0.6
⟨1/2 Tr V_l⟩

Fig. 7

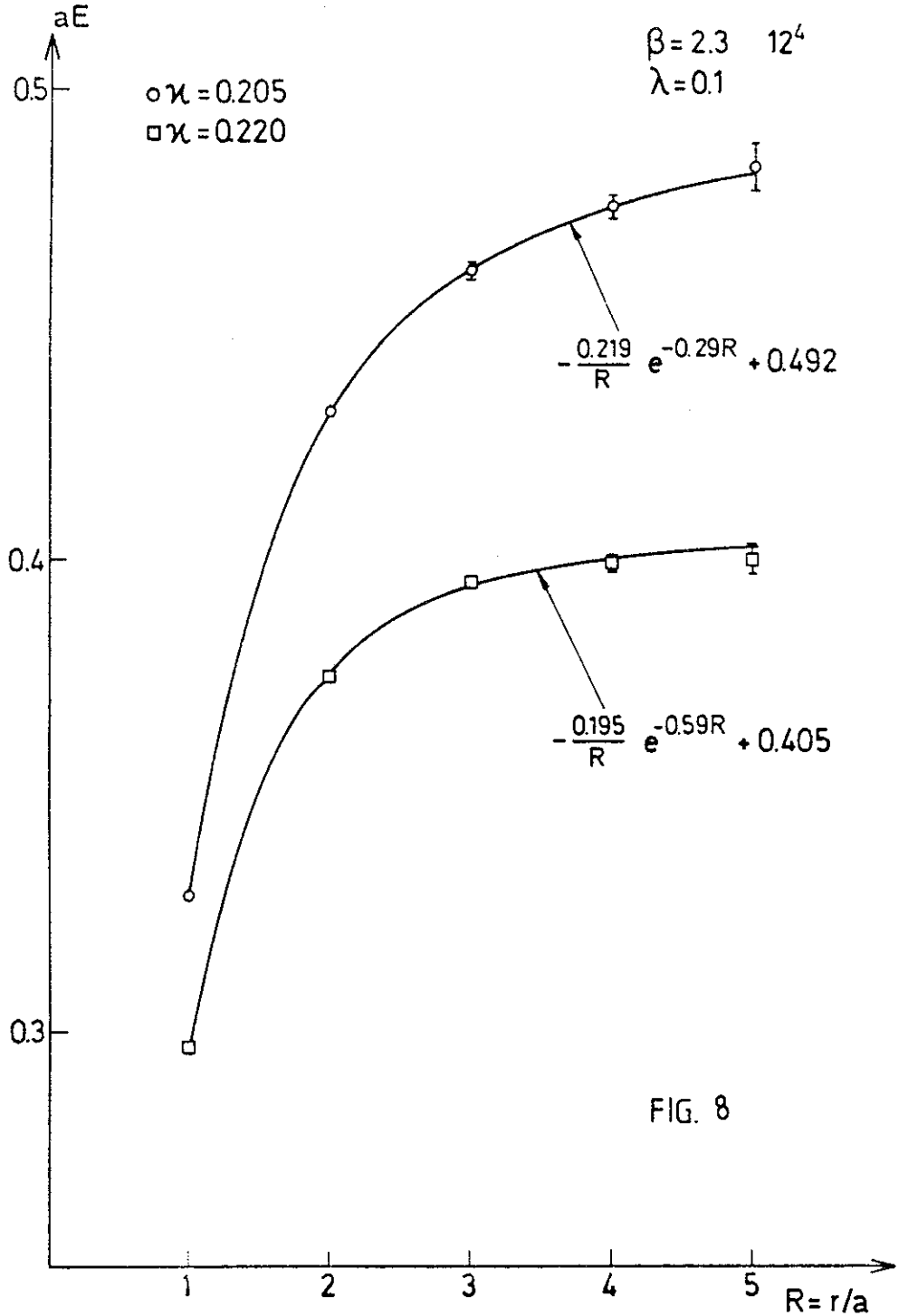
aE
β = 2.3 12^4
λ = 0.1
○ κ = 0.205
□ κ = 0.220
$-\frac{0.219}{R} e^{-0.29R} + 0.492$
$-\frac{0.195}{R} e^{-0.59R} + 0.405$
0.5
0.4
0.3
1
2
3
4
5
R = r/a

FIG. 8

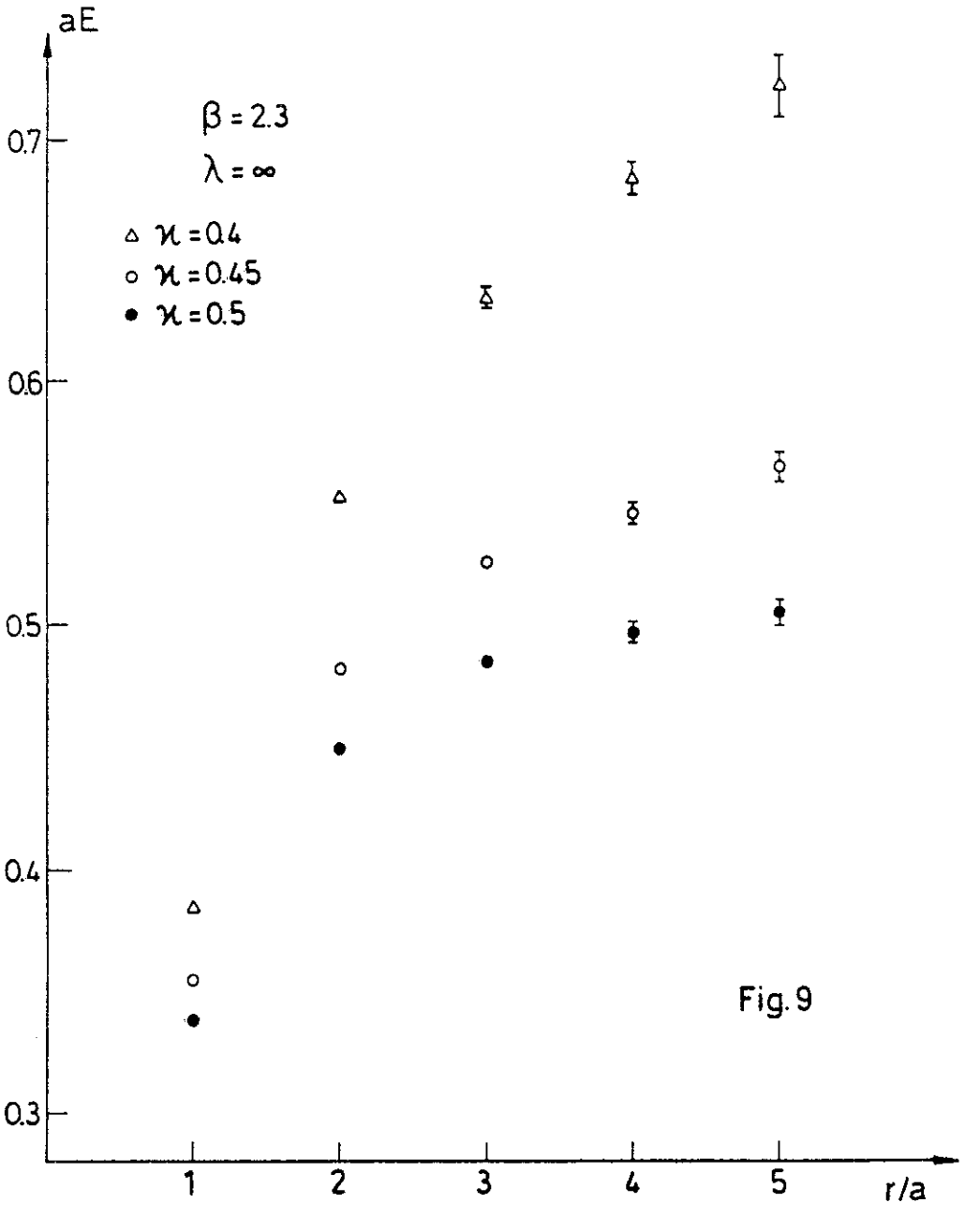
aE
β = 2.3
λ = ∞
△ κ = 0.4
○ κ = 0.45
● κ = 0.5
0.7
0.6
0.5
0.4
0.3
1
2
3
4
5
r/a

Fig. 9

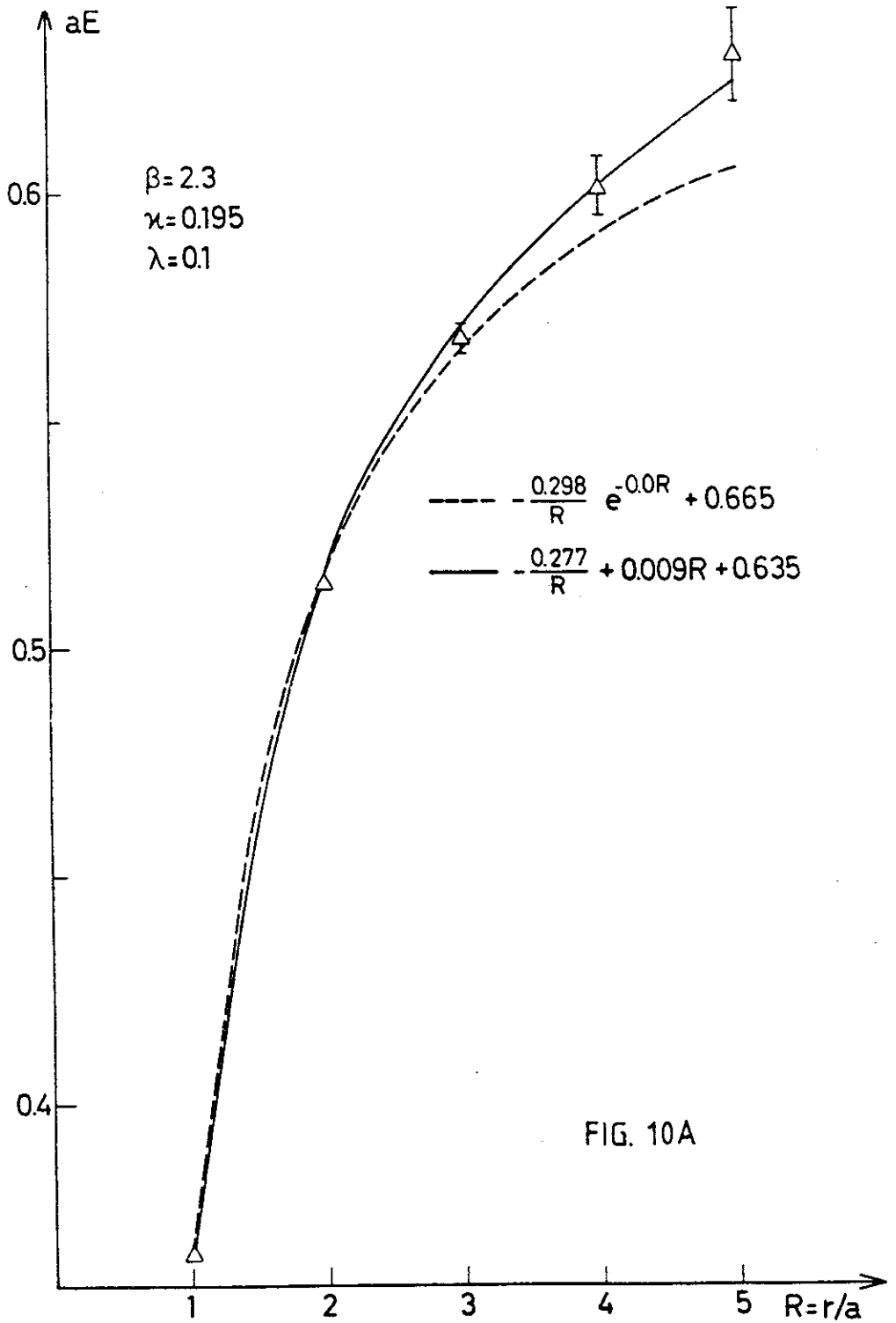

FIG. 10A

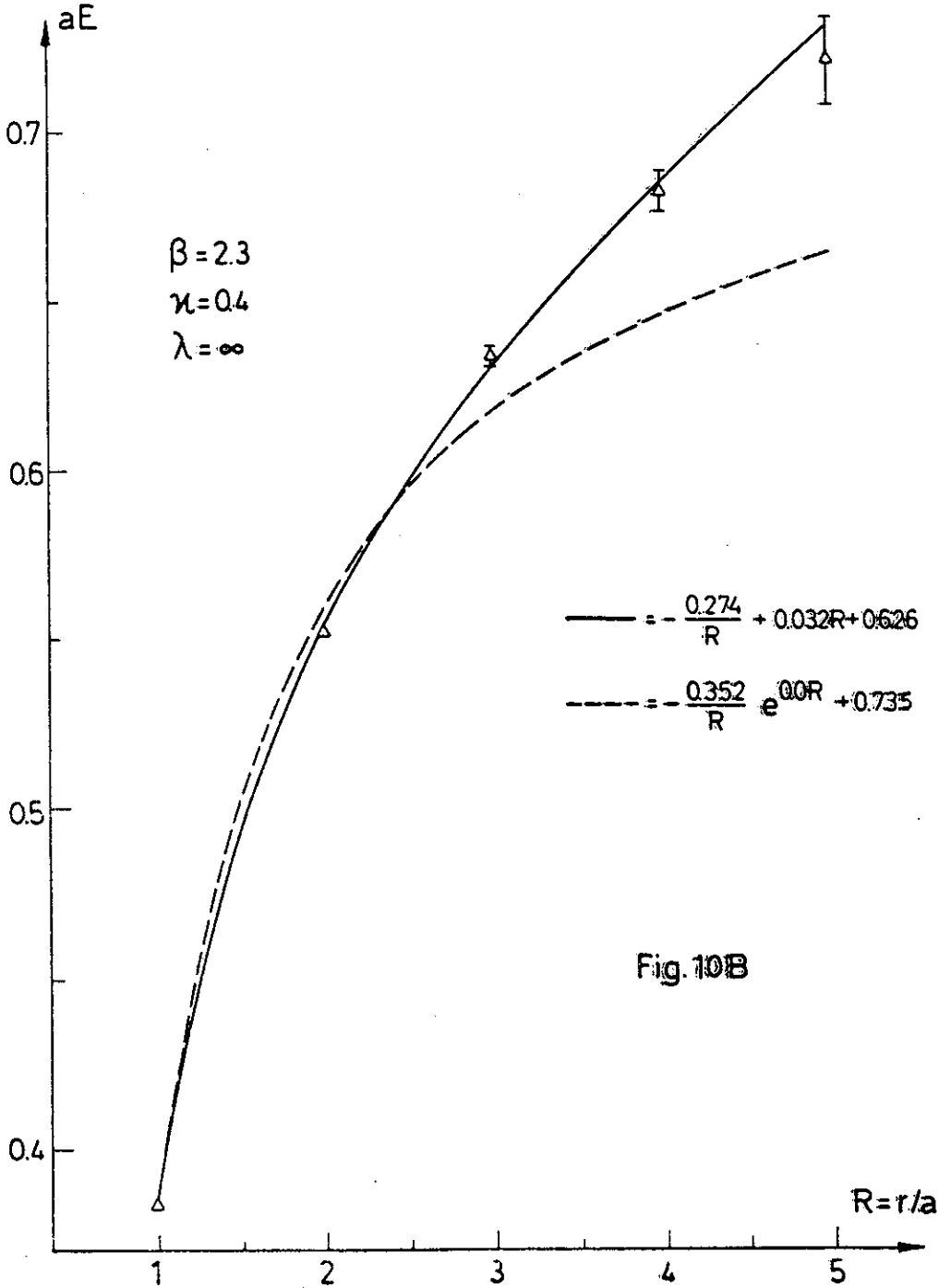

Fig. 10B

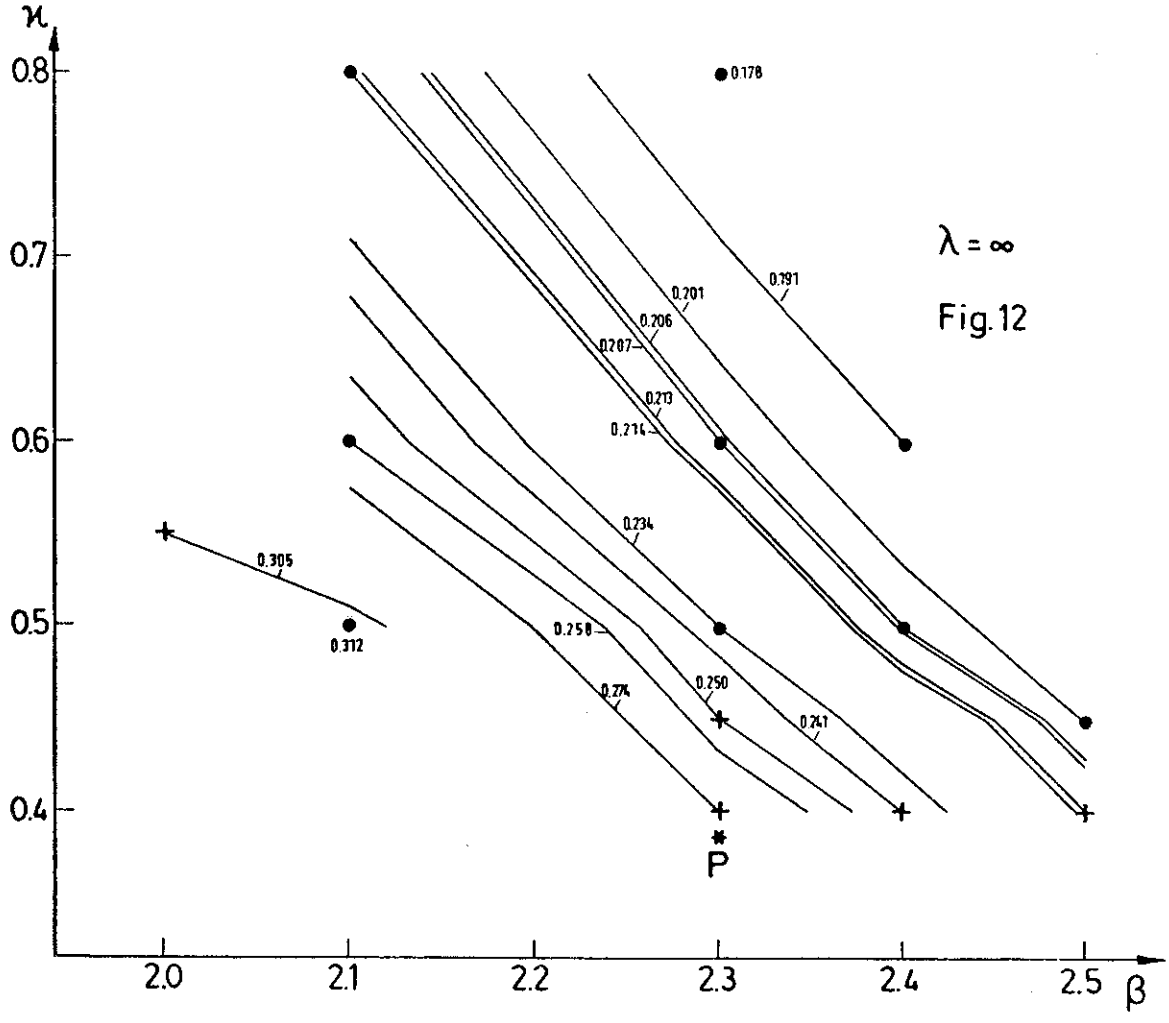

$\lambda = \infty$

Fig. 12

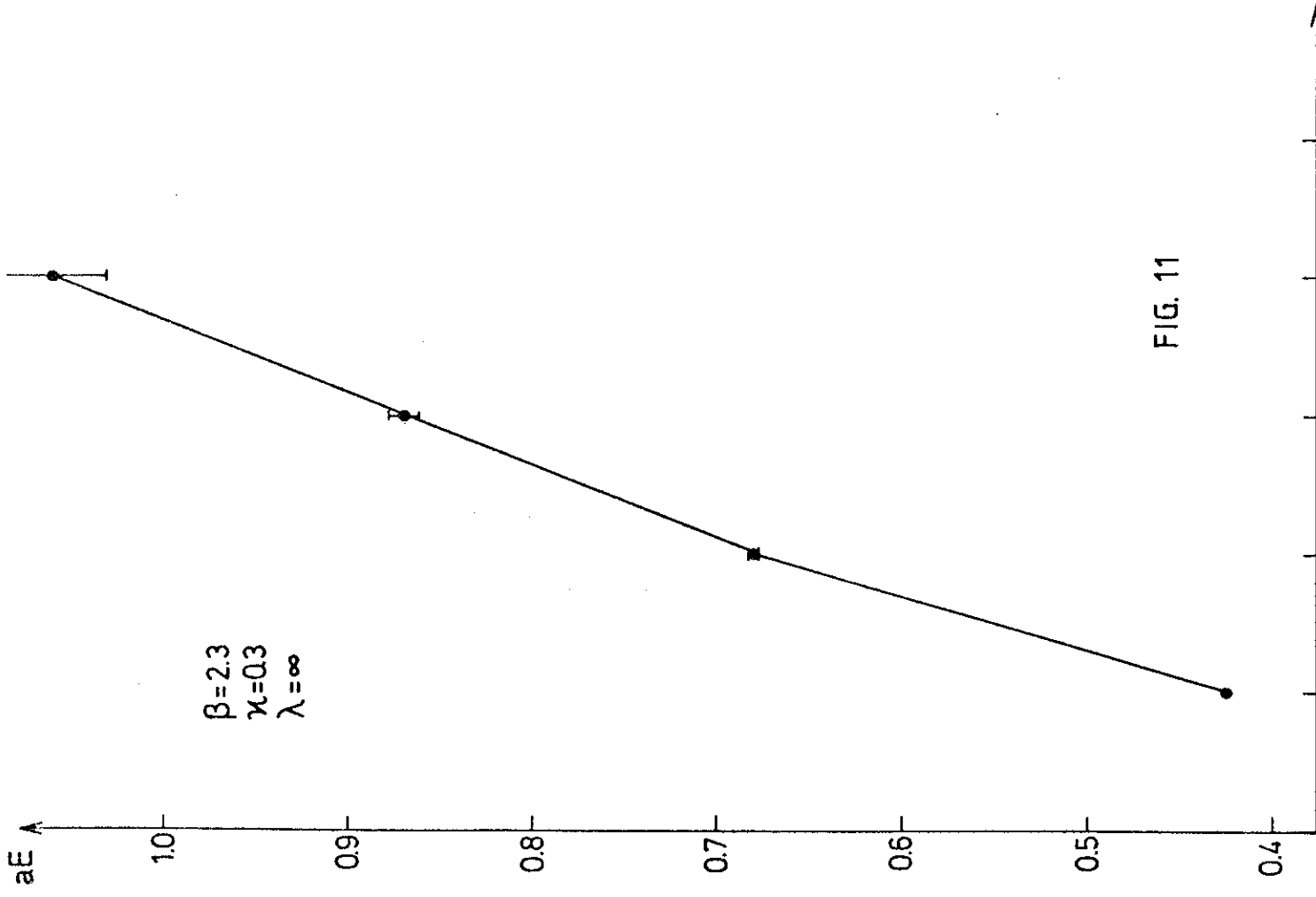

FIG. 11

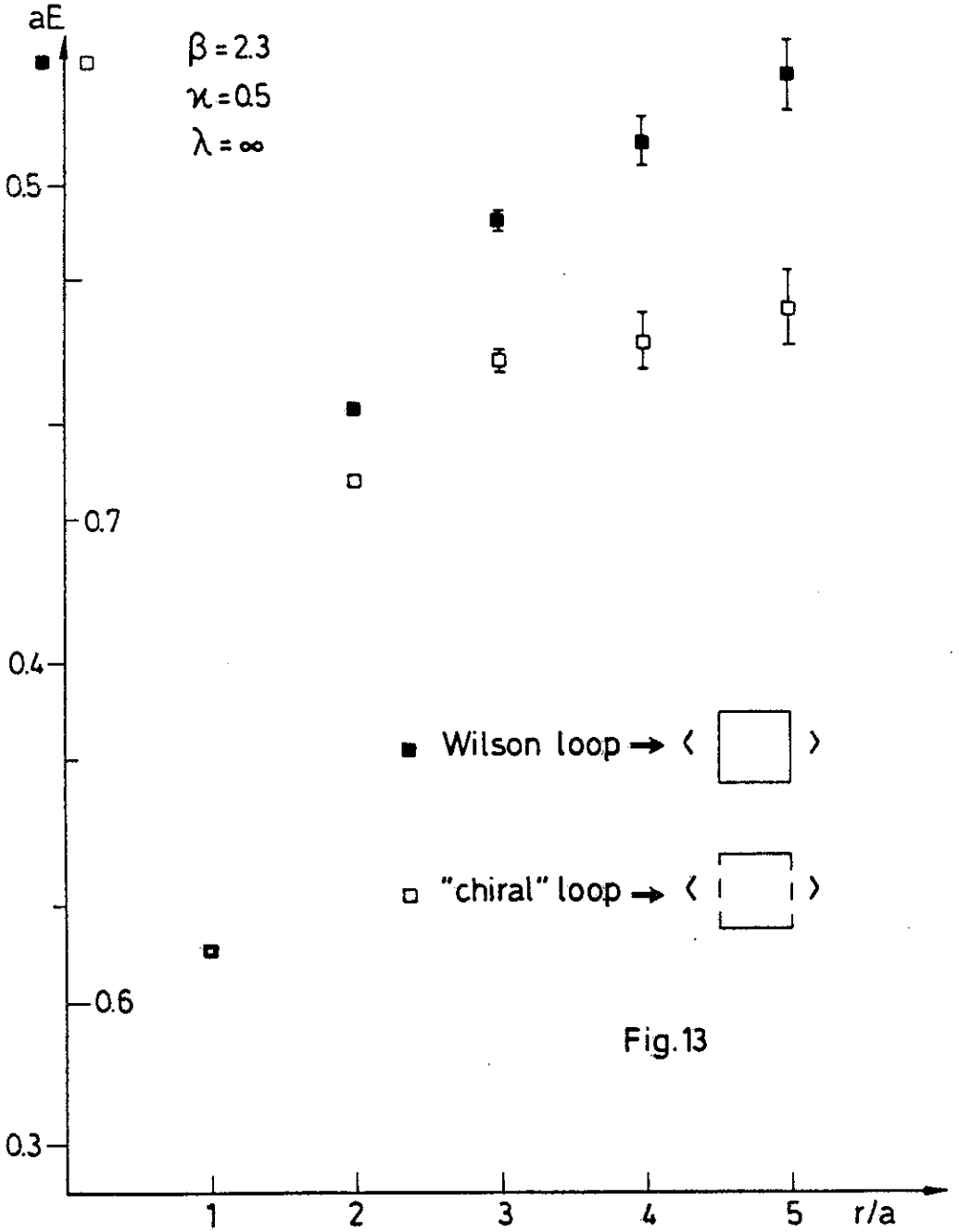
aE
β = 2.3
κ = 0.5
λ = ∞
0.5
0.7
0.4
0.6
0.3
1
2
3
4
5
r/a
Wilson loop →
"chiral" loop →

Fig. 13

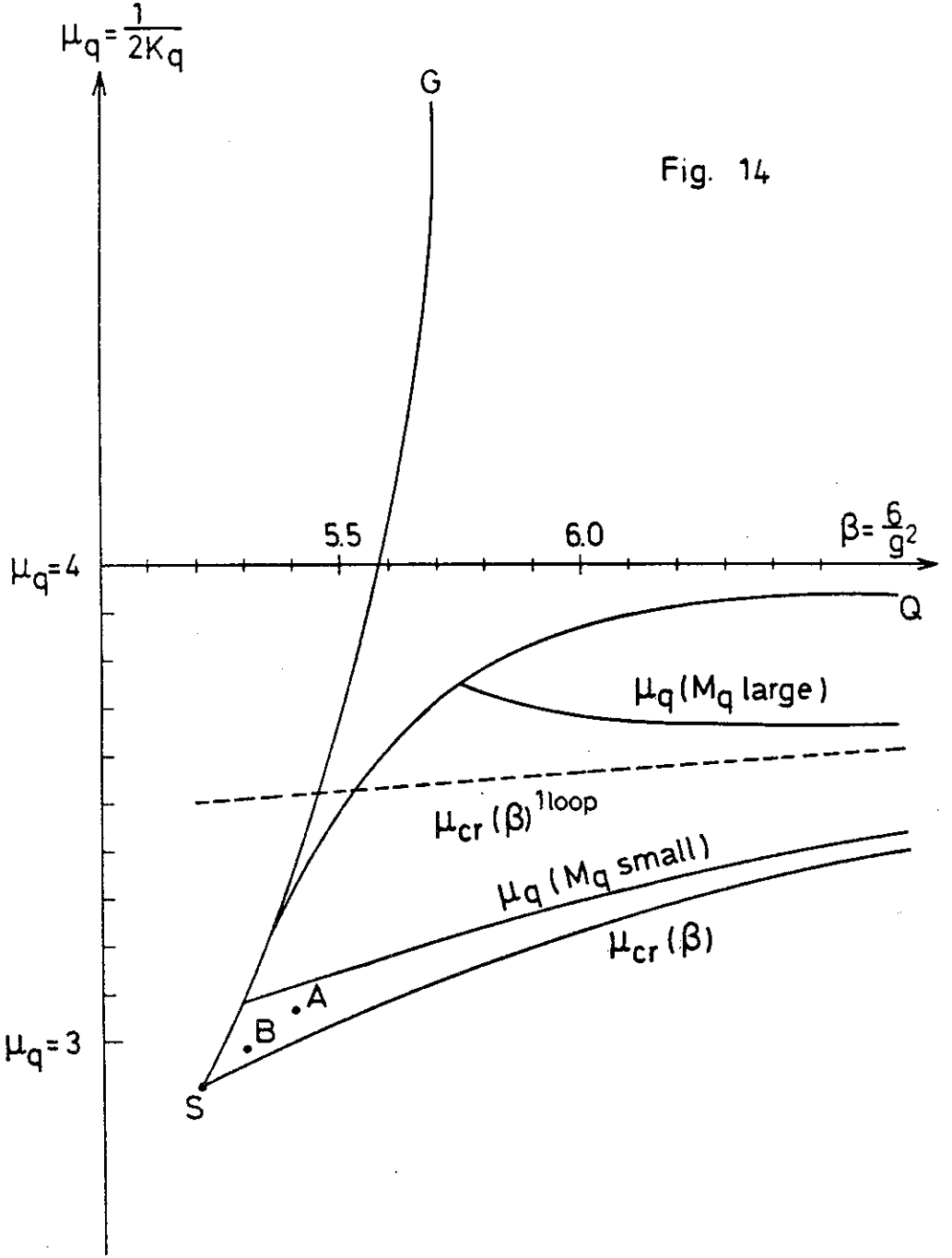
$\mu_q = \frac{1}{2K_q}$
G
5.5
6.0
$\beta = \frac{6}{g^2}$
$\mu_q = 4$
Q
μ_q (M_q large)
$\mu_{cr}(\beta)^{1loop}$
μ_q (M_q small)
$\mu_{cr}(\beta)$
A
B
$\mu_q = 3$
S

Fig. 14

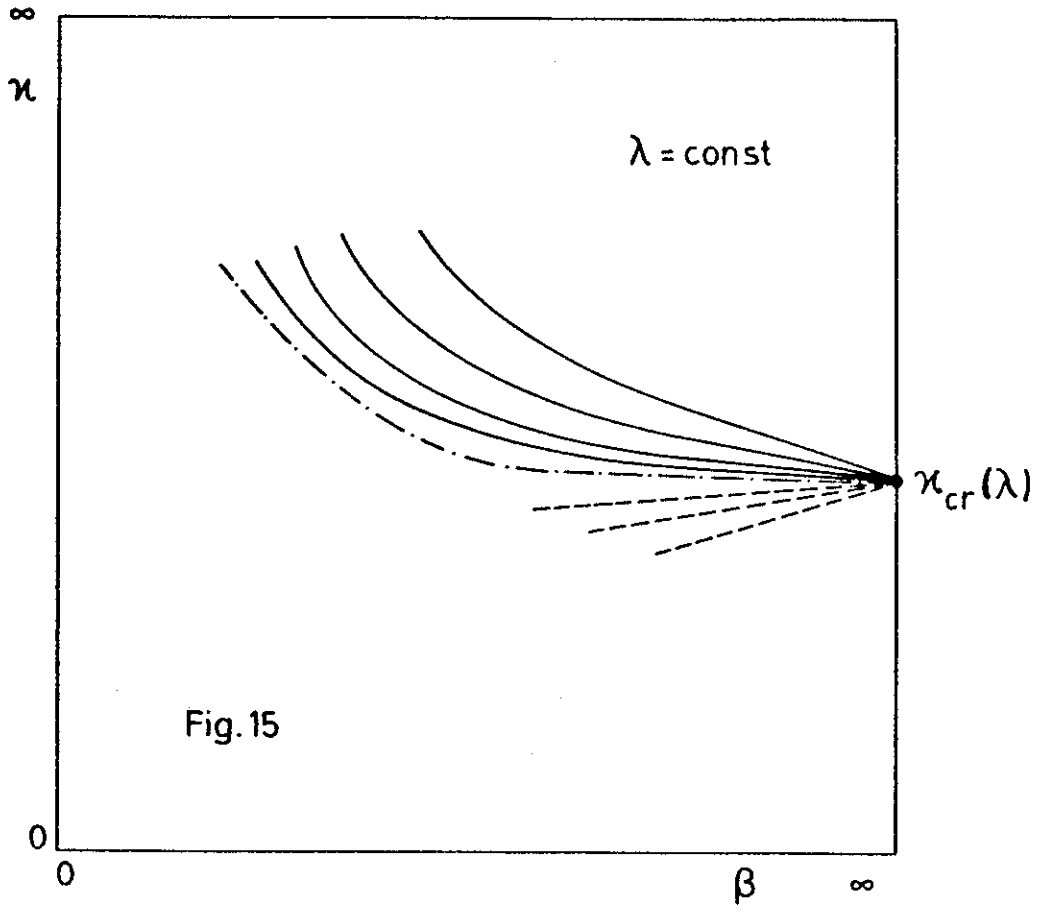

Fig. 15